January 2017

Failure Analysis Of Rotating Equipment Using Vibration Studies And Signal Processing Techniques

Ashkan Nejadpak

FAILURE ANALYSIS OF ROTATING EQUIPMENT USING VIBRATION STUDIES AND SIGNAL PROCESSING TECHNIQUES

by

Ashkan Nejadpak

A Thesis

Submitted to the Graduate Faculty

Of the

University of North Dakota

in partial fulfillment of the requirements

for the degree of

Master of Science

Grand Forks, North Dakota

June
2017

This thesis, submitted by Ashkan Nejadpak in partial fulfillment of the requirements for the Degree of Master of Science from the University of North Dakota, has been read by the Faculty Advisory Committee under whom the work has been done and is hereby approved.

Cai Xia Yang, Chair

Marcellin Zahui

Meysam Haghshenas

This thesis is being submitted by the appointed advisory Committee as having met all of the requirements of the School of Graduate Studies at the University of North Dakota and is hereby approved.

Wayne Swisher
Dean of the School of Graduate Studies

Date

PERMISSION

Title Failure Analysis of Rotating Equipment Using Vibration Studies and Signal Processing Techniques

Department Mechanical Engineering

Degree Master of Science

In presenting this thesis in partial fulfillment of the requirements for a graduate degree from the University of North Dakota, I agree that the library of this University shall make it freely available for inspection. I further agree that permission for extensive copying for scholarly purposes may be granted by the professor who supervised my thesis work or, in her absence, by the Chairperson of the department or the dean of the School of Graduate Studies. It is understood that any copying or publication or other use of this thesis or part thereof for financial gain shall not be allowed without my written permission. It is also understood that due recognition shall be given to me and to the University of North Dakota in any scholarly use which may be made of any material in my thesis.

Signature Ashkan Nejadpak

Date 6/21/2017

TABLE OF CONTENTS

LIST OF FIGURES

LIST OF TABLES

ACKNOWLEDGEMENTS

I would like to thank my advisor, Dr. Cai Xia Yang, for her guidance, generous support, and patience over the course of the past two years. I would also like to express my sincere appreciation to Dr. Marcellin Zahui, and Dr. Meysam Haghshenas for serving as my thesis committee.

Special Thanks to my parents and my brother for their continuing support, and encouragement.

ABBREVIATIONS

FFT	Fast Fourier Transform
STFT	Short Time Fourier Transform
RMS	Root Mean Square
PCA	Principal Components Analysis
KNN	k_Nearest Neighbor
SVD	Singular Value Decomposition
MFS	Machinery Fault Simulator
AE	Acoustic Emissions
MCSA	Motor Current Signature Analysis
ANN	Active Neural Network
MMF	Magnetic Motive Force
BPFO	Ball Pass Frequency of Outer Ring
BPFI	Ball Pass Frequency of Inner Ring
FTF	Fundamental Train Frequency
BSF	Ball Spin Frequency
TIR	Total Indicator Reading
AI	Artificial Intelligence
FMEA	Failure Mode and Effects Analysis

ABSTRACT

This thesis focuses on failure analysis of rotating machines based on vibration analysis and signal processing techniques. The main objectives are: identifying machine's condition, determining the faults specific response, creating methods to correct the faults, and investigating available statistical analysis methods for automatic fault detection and classification. In vibration analysis, the accelerometer data is analyzed in time and frequency domain which will determine the machine's condition by identifying the characteristic frequencies of the faults. These fault frequencies are specific for each type of machine's faults. Therefore, they are referred to as faults' signatures. The most common faults of the rotating machines are unbalanced load torque, misaligned shaft, looseness, and bearing faults. The second objective is to find correction methods for rectifying the faulty situations. Therefore, correction methods for the unbalanced condition are comprehensively studied and a novel method for balancing an unbalanced rotor is developed which is based on image processing methods and results in lowering machine's vibrations. Another objective of this research is to collect huge amount of vibration data and implement statistical data analysis methods to categorize different machine's conditions. Therefore, principal components analysis, K-nearest neighbor, and singular value decomposition are implemented to identify different faults of the rotating machines automatically. The statistical methods have demonstrated high precision in classifying different faulty situations. Fault identification at early stages will enhance machine's health and reduces the maintenance costs significantly. The statistical methods are easy to implement, and have disaffected the need for an expert maintenance engineer and will identify the machine's fault automatically.

CHAPTER 1

INTRODUCTION

1.1 Overview

Rotating machines are widely used in various fields of industry. Condition monitoring of these equipment is vital in order to avoid catastrophic failures. Condition monitoring via vibration analysis is one of the most accurate and cost effective techniques for determining the state of the equipment [1]. Excessive vibrations would cause fatigue and affect the performance of the machine. Therefore, it's desired to reduce the machine's vibrations as much as possible. The structural vibration is measured with electronic sensors called accelerometers. There are other transducers available such as displacement and velocity probes. However, acceleration data can be analyzed in high frequencies up to 20 KHz, while the displacement and velocity data can be analyzed in lower frequencies in range of 1500Hz. The accelerometer data presents the vibration response of the system in time domain. Vibration data in time domain provides valuable information about vibration's maximum amplitude, period, and decay rate. However, using solely the time domain data, it is not possible to identify the type of machine's faults precisely. Therefore, using signal processing methods, the vibration data is analyzed in frequency domain. The most common signal processing method is Fourier

Transform. Fourier Transform indicates that any periodic signal can be represented as a series of sine waves [2]. Fast Fourier Transform (FFT) is an optimized version of Fourier Transform which is mainly used through this thesis. FFT has some advantages compared to other techniques; it can be used for analyzing larger amounts of data and it is more computationally intensive. There is one drawback though, FFT only demonstrates the results in frequency domain and it does not provide any information about the vibration data in time domain. Therefore, Short Time Fourier Transform (STFT) is used to display the vibration data in time and frequency domain and therefore can be used to analyze transient signals [3]. The effects of different faults on vibration response of the system are investigated using the proposed signal processing methods.

Motor's faults can be categorized into two groups of mechanical and electrical faults. Mechanical faults can be investigated thoroughly using accelerometer data. However, electrical faults are not identified precisely using solely the accelerometer data, and could be mistaken with other types of faults, a specific case is studied in chapter three which demonstrates that a damaged winding could be mistaken for a lenient unbalanced situation [4]. In order to achieve high accuracy in the measurements, the experiment setups have been designed to provide adequate repeatability when introducing different electrical or mechanical faults to the machine.

In this thesis, the frequency spectrums of different faults are investigated. Correction methods for reducing machine's vibrations are presented. Different statistical methods are implemented to categorize the system's faults. The final conclusions are made based on the fault's characteristic frequencies and the statistical approaches.

1.2 Objectives

The main objective in this research is to identify the faults present in the rotating machines. For this purpose, various condition monitoring techniques are studied. The comparisons between different monitoring techniques are made based on their accuracy in identifying the most common faults of rotating machines and the convenience of the employed monitoring equipment. The results demonstrate that vibration analysis has high level of accuracy in finding failure types with inexpensive accelerometer sensors available.

The most basic form of vibration monitoring is to consider the trend of the overall vibration data in time domain to look for increases or instability in vibration's amplitudes. In order to find the exact corresponding failure in the machine, the data should be studied in frequency domain. Therefore, the second objective is to find a signal processing method which is easier to implement, and provides most comprehensive information on the condition of the machine. Nowadays, the dynamic signal analyzers provide real-time processing of the acquired signals. It is not accurate to use only one signal processing method for all types of faults diagnosis. For different inquiries, Fourier Transform is implemented because it can determine the characteristic fault frequencies accurately.

It is important to design permanent experiment setups to be able to take the measurements repetitively in equivalent settings. There are two settings that have to be initiated for each experiment. First one is the software settings. In this study, National Instrument Sound and Vibration Assistant software is used for data analysis. Averages of the acquired data are taken to improve the quality of measurements and suppress the

background noise. A Hanning window is applied to cover for 'leakage', which is referred to the effect of signal energy fading in a wide frequency range when the signal is not periodic. The vibration amplitude is represented in Root Mean Square (RMS) units. The RMS value is expressed from zero to 70.7 % of the peak amplitude for a single frequency. Second setting is associated with modifying operating speed of the machine, introducing the exact amounts of failures, whether it is the amount of unbalanced mass to the extent of misalignment created. Moreover, there are different mounting methods for the accelerometers which affect the measurements. The frequency limit of each mounting method is presented in Table 1.1 [5].

Table 1.1: Frequency limit for accelerometer measurements based on mounting methods

Mounting Method	Frequency Limit (Hz)
Hand held	500
Magnet	2000
Adhesive	2500-4000
Stud	6000-10,000

Another objective is to find some methods to categorize different faults automatically. A method which can identify an unknown situation based on the training datasets recorded. As we are facing large amount of data, different statistical methods are investigated to find best procedure that can classify different faulty conditions with high accuracy. Three approaches are implemented and modified so they can precisely achieve the main goal of this research which is fault detection of rotating machines. Investigated statistical methods include: Principal Components Analysis (PCA), K-Nearest Neighbor

(KNN), and Singular Value Decomposition (SVD). The applicability of these methods is investigated thoroughly in the text. Moreover, in faults correction section, a balancing method is developed based on accelerometer data and videos recorded from the rotating shaft. Using image processing methods, the exact amount and location of the correction mass is obtained. Results demonstrated that the developed method has high levels of precision. The future plan is to commercialize this balancing technique via developing a smart phone application.

1.3 Orientation

The thesis includes six chapters. In first chapter a brief overview of condition monitoring via vibration analysis and objectives of the research are presented. In chapter 2, a comprehensive literature review on condition monitoring, vibration studies, novel condition monitoring approaches, and implementation of different statistical methods in vibration analysis and fault diagnosis are conducted.

In chapter 3 three experiment setups used for condition monitoring of rotating machines are discussed. One setup is the Machinery Fault Simulator (MFS). This simulator has the opportunity to model all mechanical faults, however, is mainly used to model the misalignment condition. The others setup was used to model both mechanical and electrical faults. Next, the acquired signals processed through NI Sound and Vibration Assistant software are investigated to find the characteristic fault frequencies corresponding to each faulty situation.

Chapter 4 provides vibration control methods for the unbalanced condition. A novel methodology based on image processing techniques is developed. The vibration data is

recorded twice; one from the original unbalanced situation, another after a test mass is added to the rotor. From these data, the maximum vibration's amplitude is provided. In both vibration recording phases, a video is also captured from the rotating shaft. The video is analyzed to find the location of a randomly marked area when the sinusoidal vibration signal reaches maximum. Based on two marker locations and the accelerometer data, the amount and location of the correction mass can be found.

In chapter 5, vibration data is analyzed using different statistical methods such as PCA, KNN, and SVD. It is demonstrated that using these methods, it is possible to categorize and identify the failure types and predict their severities. The conclusions, contributions, and the scope for future research in area of condition monitoring and vibration analysis are discussed in chapter 6.

CHAPTER 2

LITERATURE REVIEW

2.1 Overview

In this chapter, an extensive literature review on condition monitoring of rotating machines is performed. The topics studied mainly include different condition monitoring methods such as vibration analysis, infrared thermography, acoustic emissions, and electric current monitoring. Moreover, novel developments in this field are investigated. These developments include exploring new vibration analysis methods using image processing techniques or implementing machine learning algorithms for fault detection.

2.2 Condition Monitoring

In industrial applications the upkeep of the machine can be enhanced through equipment's condition monitoring. While the condition of the machine is known at all times, the unexpected process halts due to machine's failures can be avoided, therefore, the efficiency of the production process will increase significantly. Moreover, it is possible to plan for maintenance way before the machines fail [6]. There are several condition monitoring methods available. Vibration analysis, lubricant analysis, infrared thermography, electrical monitoring, and acoustic emissions are the most common

monitoring techniques available [7]. The most effective condition monitoring approach would be when two or more of the mentioned techniques are integrated and used together.

2.2.1 Vibration Analysis

All machines vibrate, whether they are in healthy condition or when a fault is present in the machine. These vibrations are related to a periodic occurrence in the machine. Vibration analysis has some advantages compared to other monitoring techniques. First, it demonstrates the occurring failure immediately. Second, the major signal processing methods can be applied to the vibration signals [8]. The last and most important advantage is that the mechanical procedures in the rotating machine each produce energies at different frequencies. Therefore, the frequency spectrum of vibration data can display more detailed information on condition of different parts of the machine [7]. A vibration analysis system consists of the following parts [9]: a vibration signal transducer (accelerometer, displacement or velocity probes), a dynamic signal analyzer, analysis software, and finally a computer for data analysis and storage. Overall, vibration analysis can be used to improve the machine's reliability, by providing detailed information on health condition of machine's components. Randall [10] investigated vibration analysis to study gear and bearing fault frequencies. Investigating the vibration response of misaligned rotor of different machines using signal processing methods [11, 12] demonstrates that vibration analysis has achieved decent precision in identifying the most common machine faults.

2.2.2 Infrared Thermography

Electrical machines have benefited from this monitoring method significantly. With thermal imaging cameras it is possible to create a temperature map for machine's components like bearings and couplings. One advantage of this method is that it requires less training dataset compared to other methods [7]. Moreover, it's a non-contact condition monitoring tool and can be used to identify mechanical and electrical faults. However, it suffers from high cost of infrared cameras. Lim et. al. [13] used infrared thermography to identify the rotating machineries failures and found satisfactory levels of accuracy compared to vibration monitoring methods.

2.2.3 Acoustic Emissions

Ultrasonic and acoustic emissions (AE) use similar approaches as vibration analysis; even the transducers are mounted on the same location as the accelerometer sensors. Acoustic signals are studied to identify defects in bearings [14] and investigating gear failures [15]. Loutas et. al. [16] argued that the combination of vibration analysis and AE would result in a more effective condition monitoring of rotating machinery.

2.2.4 Electrical Monitoring

Electrical condition monitoring methods such as current or voltage monitoring provide the most precise data about the electrical faults present in the system. However, they lack accuracy for identifying and distinguishing different mechanical faults [4]. Neelam Mehala [17] has discussed electrical monitoring based on Motor Current

Signature Analysis (MCSA) for most electrical faults and bearing faults of the induction motors.

2.2.5 Lubricant Analysis

Lubricant analysis is a very common technique in condition monitoring. However, for condition monitoring of electric motors, it does not provide decent results exclusively. This method becomes more useful when combined with other monitoring techniques such as vibration analysis and acoustic emissions [16].

2.3 Statistical Analysis

When the vibration data is collected from the machine, using signal processing methods, the vibration data can be analyzed in frequency domain. After recording frequency responses of different healthy and faulty conditions with various severities and operating under different rotational speeds, a massive database is collected. Therefore, it is necessary to define feature extraction methods to accelerate fault diagnosis and be able to automatically detect machine's condition. Consequently, in recent studies the statistical approaches are considered to find the best classifying technique.

Plante et. al. [18] and Lachouri et. al. [19] used Principal Components Analysis approach to categorize rotating machine's faults based on failures types and their severities. PCA is a statistical approach mainly used in image processing when large amount of data is present.

The motors faults are investigated based on their acoustic signals using K-Nearest Neighbor in [20]. Lei et. al. [21] identified the crack levels of the gears based on KNN classifiers. Safizadeh et. al. [22] studied bearing fault diagnosis based on accelerometer data which achieved more accurate precision in fault detection using KNN classifiers.

Another feature extractor studied is Singular Value Decomposition technique. Yang et. al. [23] used wavelet transform of the vibration data with the SVD method to detect different bearing faults. Using the singular value decomposition technique, the failure on different complex structures can be identified at early stages [24]. Based on the three methods discussed, it's clear that in recent years more studies are performed on using different statistical methods for failure detection and classification.

2.4 Novel Condition Monitoring and Data Analysis Methods

As mentioned before, the statistical methods implementation for data analysis is amongst the recent developments within condition monitoring and vibration analysis studies. Several studies have studied the combinations of the monitoring tools to achieve the best condition monitoring technique [16].

Other researchers have focused on fault diagnosis based on Artificial Neural Network (ANN). ANNs have been commonly implemented for fault diagnosis of rotating machines [25]. Artificial neural networks can be used for condition monitoring of gear boxes [26] and for fault diagnosis of rolling element bearings [27].

Machine vision applications have increased significantly during the past few years. In image processing applications, feature detection and extraction are among the most

useful tools which can be related to fault diagnosis methods. Zhang et. al. [28] used morphology for diagnosis of different types of bearing failures. The most recent studies have focused on amplifying small motions and color variations [29-31]. This technique uses different image processing methods to identify the smallest amounts of motion. The motions are then amplified, and the results could be used to achieve the vibration response of the system without the accelerometer sensors. Based on their developed method, different types of diagnostic tools can be developed, Davis et. al. [32] identified material properties based on the motions detected in the captured video.

2.5 Chapter Summary

In this chapter, a literature review for the most common condition monitoring methods is presented. Different statistical methods were investigated to be implemented for development of an automatic fault detection scheme. Finally, the latest advanced condition monitoring techniques are investigated. Recent developments in computer vision and image processing techniques have demonstrated high accuracy in identification of smallest vibrations not with accelerometer sensors but using solely the video recorded by a camera. An important remark from literature review was the high necessity of a low-cost and reliable condition monitoring technique to ensure the operation consistency of the induction machines.

CHAPTER 3

VIBRATION DATA ANALYSIS

3.1 Overview

Scheduled and break down maintenances are commonly used by industries, but both tend to incur much higher costs. Predictive or Condition-Based Maintenance based on known condition is used to predict (and therefore assist in avoiding) unplanned equipment failures. During observation of the vibration modes, a relationship was found between the ranges of natural frequency of vibration and the failure modes. By measuring and analyzing measured vibration data, engineers are able to retrieve valuable information on the status of the equipment, and predict machine failure patterns and plan timely maintenance operations. To progressively extend the time between failures for the monitored equipment, the trend of vibration in frequency domain needs to be observed frequently. The trend of the spectrum will provide information on what type of faults are present within the system, the severity of the fault, and could be implemented to determine the remaining lifespan of the faulty component.

Understanding the concepts behind vibration data allow engineers to detect faults and predict failures caused by equipment defects, or deterioration such as unbalanced rotors, bearing defects, a lack of lubrication, coupling issues, and misaligned axles before

they lead to catastrophic failure. To understand how vibration analysis can be used to identify motor faults, one must first understand that all mechanical systems vibrate. This vibration retains a unique signature which, given proper analysis, can tell an operator how the system is responding to its operating conditions. Altering operating conditions may reveal different signatures yet, at the same time, patterns emerge suggesting a specific problem within the system. Over time, certain patterns can become more evident suggesting a fault is likely to occur if left uncorrected. Recognizing and categorizing these patters before equipment failure is the objective of fault detection and predictive maintenance, and allows corporations and industries to reduce spending in equipment repair and replacement. This concept correlates to the method of predictive based maintenance.

In this chapter, three experiment setups are employed to acquire vibration signal for different faults and a setup is designed for acquiring the electrical signals from the induction machine. Next the acquired signals are analyzed using signal processing techniques and the characteristic frequencies corresponding to the machine's faults are investigated.

3.2 The Experiment Setups

In this section, three experiment setups are designed and described. The first setup can be used to collect vibration data for the unbalanced rotor condition, bearing faults and looseness. This setup is shown in figure 3.1.

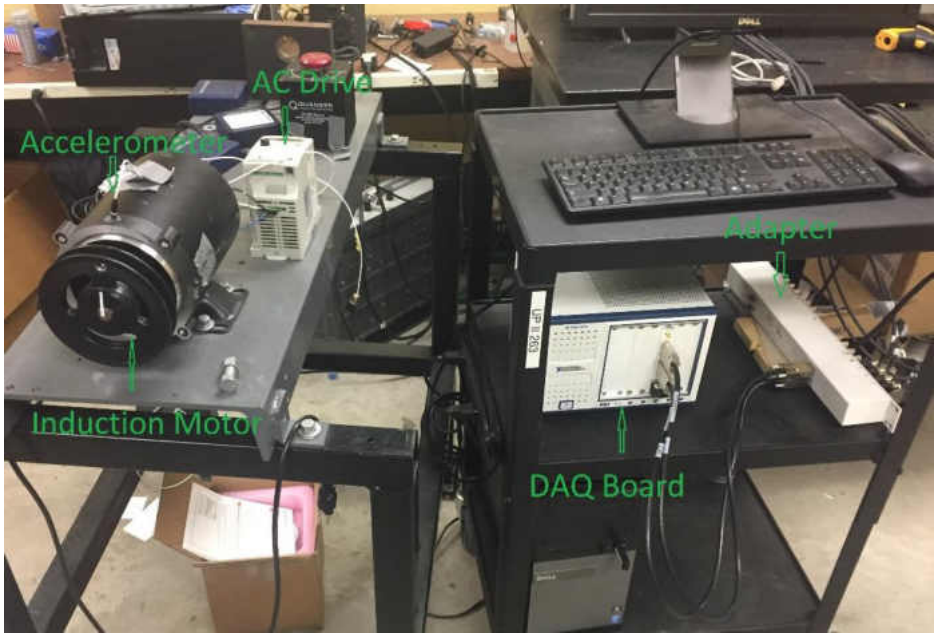

Figure 3.1: The experiment setup for obtaining vibration data.

The experimental setup shown in figure 3.1 consists of a three phase, 4 poles induction motor, an AC drive for the motor, an analog to digital converter (ADC), an accelerometer, and a NI PXIe 1073 data acquisition (DAQ) board. The output data was analyzed using a NI-PXI 4498 module on the DAQ board. The rotor was initially set to run at 30 Hz (1800 RPM). Several failure conditions, such as: damaged bearing, unbalanced load on shaft, and machine's looseness were investigated and their effects on the motor's vibration were analyzed and compared to the healthy condition. The data was analyzed using NI Sound and Vibration Assistant Software.

The second setup is used for obtaining electrical signal from the stator's current to investigate then effects of damaged stator's windings on both vibration and electrical current signals. This setup is shown in figure 3.2.

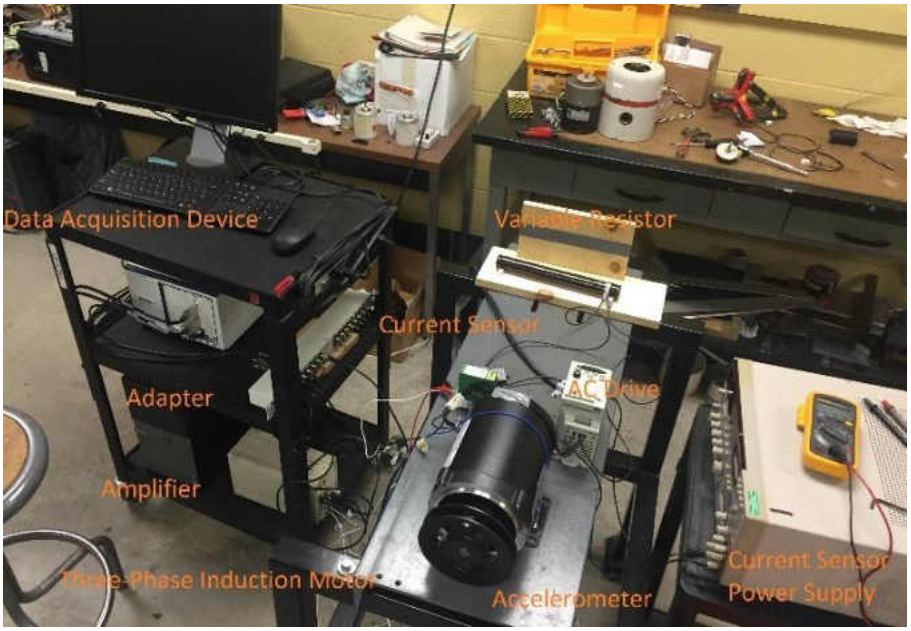

Figure 3.2: Vibration and current monitoring setup.

Figure 3.2 displays the experiment setup for acquiring both vibration and electrical current data. Here, a current sensor, a variable resistor, and a power supply for current sensor is added to the previous setup. The effects of the damaged bearing, bad wiring, and unbalanced condition on the motor's vibration and the stator's currents were analyzed and compared to the healthy condition.

The third setup has great potential in modelling several mechanical faults. Basically, the first two setups were only used because the machine's components were more accessible. Figure 3.3 displays the Machinery Fault Simulator (MFS). This setup is mainly used to investigate the effects of misaligned rotor on vibration signals.

Figure 3.3: Machinery fault simulator used as third condition monitoring setup.

In next section, different mechanical and electrical faults are inspected and their corresponding vibration responses are investigated.

3.3 Failure Analysis

The goal of this experiment was to find evidence regarding vibration patterns associated with specific electric motor faults. Specifically, the objective of the experiment was to determine the validity of using vibration analysis to conduct predictive based maintenance. Based on previous research, there are several common motor faults that can be identified using vibration analysis such as imbalance, mechanical looseness, and bearing faults [33]. Each faulty condition's severity and type can be assessed based on the amplitudes of the corresponding peaks as well as their respective locations on the

frequency spectrum. Additionally, certain types of faults can be determined based on the location where data was recorded on the equipment. In other words, some faults display a higher level of severity when the accelerometer is placed on various locations of the motor. To demonstrate the effects, different faults have on the motor's corresponding vibration levels, multiple tests were conducted on a three phase inverter duty induction AC motor.

3.3.1 Healthy Condition

First, the vibration data of a motor when there are no faults present in the machine is investigated. Figure 3.3 displays the vibration response of the healthy machine operating at 30 Hz.

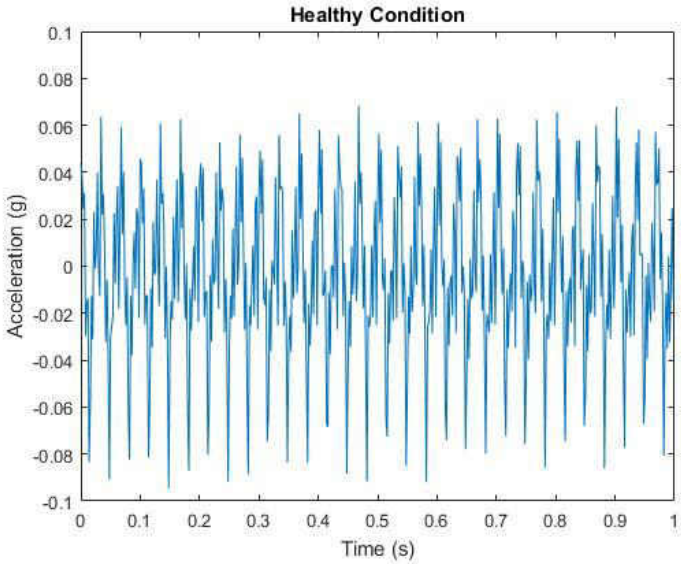

Figure 3.4: Vibration response of the healthy condition in time domain.

Figure 3.4 displays the vibration response in time domain, as mentioned before, the vibration data expressed in time domain provides information on maximum vibration's

amplitude, and period. It is clear that the maximum vibrations in healthy condition are quite low. In order to identify the condition of the machine, using FFT vibration data is brought to frequency domain. Figure 3.5 displays the linearized data in frequency domain.

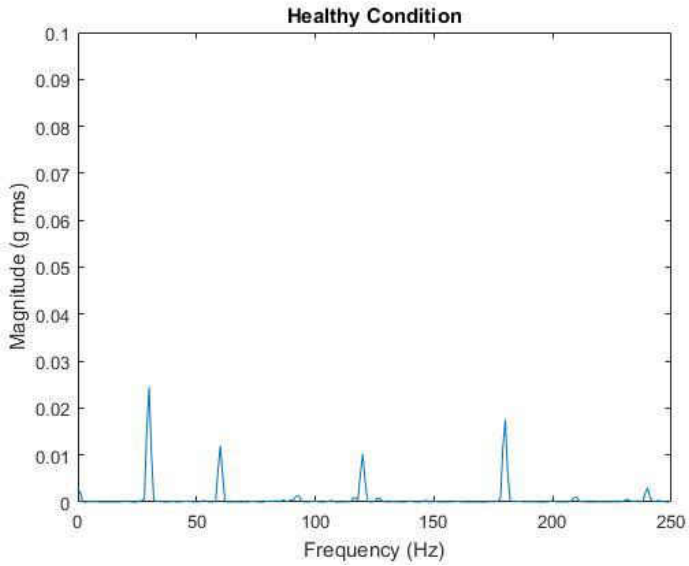

Figure 3.5: Vibration response of healthy condition in frequency domain.

Figure 3.5 shows the vibration response of the machine at healthy condition. This data resembles the acceleration signal measured in radial axis and it is not scaled or shifted. It is important to note that the magnitude is displayed in *g rms* units. This graph displays that the highest amplitude (0.025 *g rms*) arises at the operating speed of the machine which was 30 Hz. In this study, the machine's faults generate high vibration amplitudes at their characteristic frequencies and therefore throughout the text the data is mainly studied in linear form. This linear representation of the vibration data does not display the minor vibrations

Figure 3.6 displays the vibration data in logarithmic scale. The logarithmic spectrum can visualize the smallest vibrations that cannot be seen in linear format.

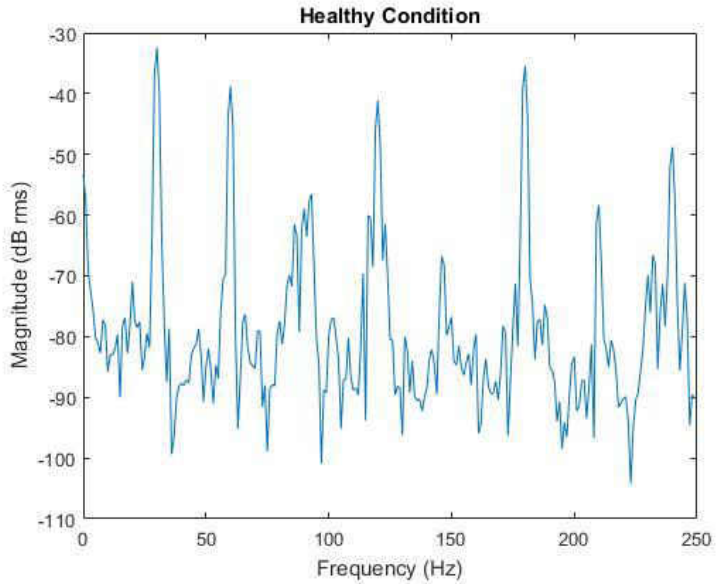

Figure 3.6: Frequency response of the healthy condition in logarithmic scale.

In linear form of figure 3.5 the vibration's amplitudes at multiples of operating speed are not shown in details. However, Figure 3.6 demonstrates how the smallest vibrations can be magnified in logarithmic scale. The decibel is the ratio of one level with respect to the reference level. For the case above, the reference is set to 1 g.

Considering the frequency spectrum via FFT method has a disadvantage which is lack of provided information regarding vibration data in time domain. Therefore, Short Time Fourier Transform (STFT) is implemented to provide a 3 dimensional vibration spectrum. Figure 3.7 displays the vibration data via STFT.

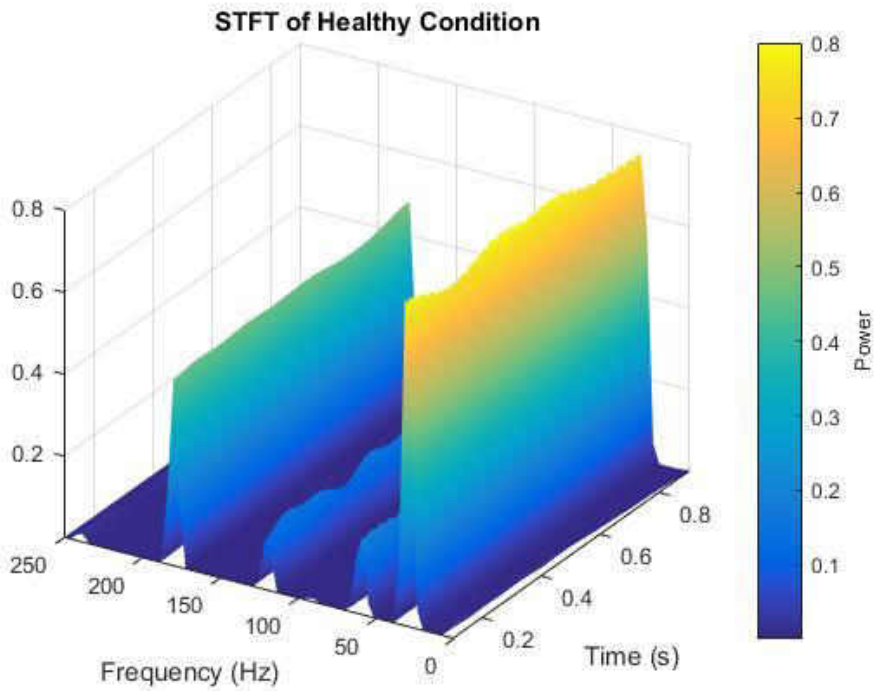

Figure 3.7: STFT of healthy condition.

Figure 3.7 displays both time and frequency information of machine's vibrations in healthy condition. The third dimension provides the power amplitudes. The distinguished waves are noticed at the vibration peaks at multiples of operating speed.

3.3.2 Unbalanced Condition

To study the unbalanced rotor condition, a steel bolt was mounted to one end of a flywheel located on the rotating shaft. According to previous research, a motor with an unbalanced rotor will display a large amplitude peak at one times the running speed [33]. Operating at 30 Hz, the motor's vibration data was recorded using an accelerometer in radial axis. Figures 3.8 and 3.9 display the frequency response of the unbalanced situation.

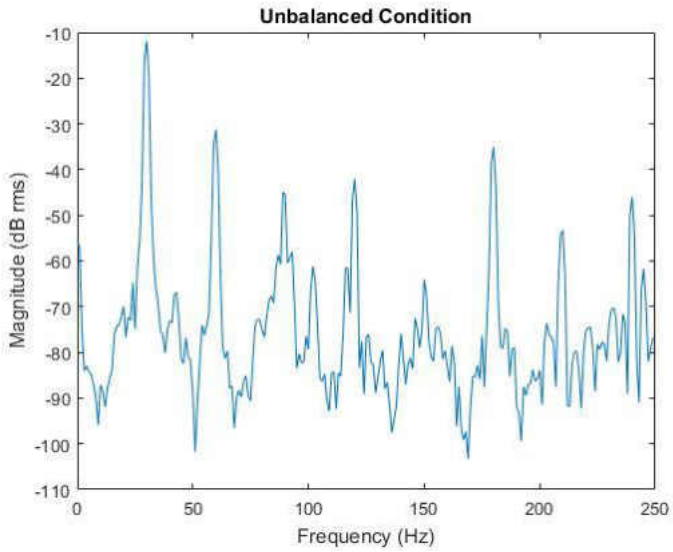

Figure 3.8: Frequency response of the unbalanced condition in logarithmic scale.

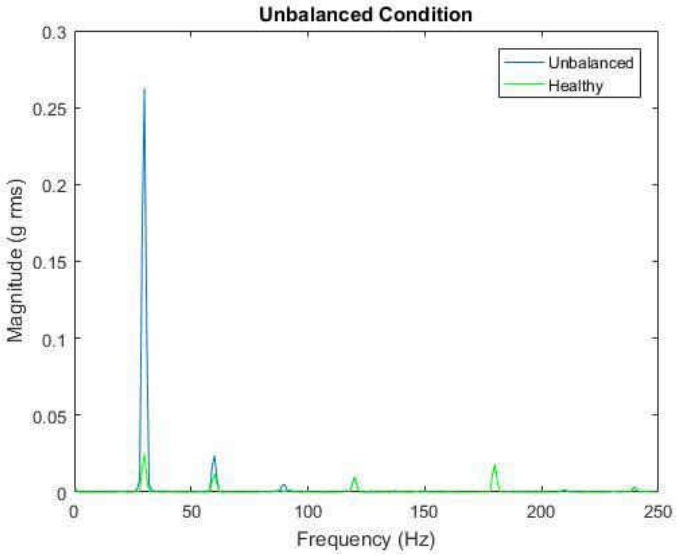

Figure 3.9: Frequency response of the unbalanced condition in linear format.

Based on figures above, several peaks appear to be present. The most notable peak is the one at 30 Hz. The 30 Hz peak correlates to the running frequency of the motor drive axle and has an amplitude of approximately 0.26 *g rms*. Compared to the 30 Hz peak of 0.025 g for the healthy condition. The 30 Hz peak of unbalanced situation vibration

response shows a substantial increase in amplitude. This observation outlines the unbalance condition. Because the motor's balanced state was the only condition altered during this experiment, it can be stated that the differences between two graphs of figure 3.9 support the presence of unbalance within the system. Therefore, it is realized that the unbalance fault condition can be associated with a large increase in the operating speed frequency. Now, let's investigate the effects of the unbalanced condition on stator's current. Figure 3.10 displays the corresponding current signal due to unbalanced condition.

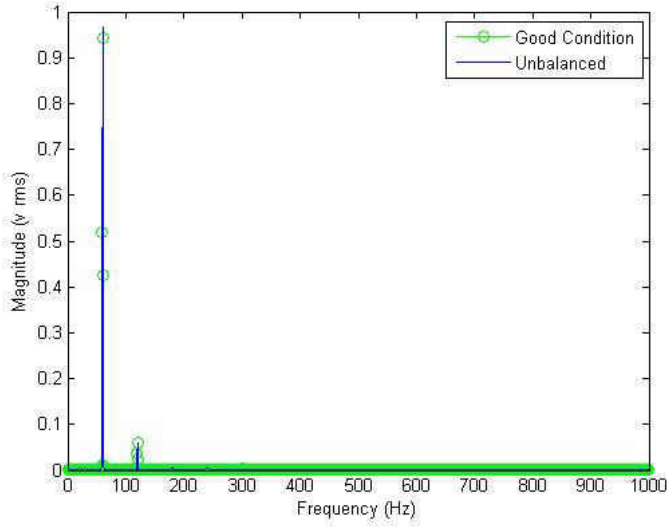

Figure 3.10: Current graph for unbalanced condition.

Figure 3.10 depicts the current transducer data; it is demonstrated that the unbalanced load condition has slightly (22 mV_{rms}) affected the amplitude of frequency response of the stator currents at 60 Hz. This demonstrates that the unbalanced rotor condition is recognized inefficiently using an electric current transducer. It is important to note that this 60 Hz value is corresponding to the speed set on the AC Drive, as the motor has four poles, its operating speed would be 30 Hz. The main reasons the current sensor

has not detected much change in the system is that the unbalanced load's weight is insignificant compared to the rotor's weight. Moreover, the system stays electrically balanced and the voltage of all three phases increases by 22 mV_{rms}. Therefore, it is driven from this experiment that the current data has not provided results as precise as the vibration data.

3.3.3 Bearing Faults

Bearing faults are considered the most common case when maintaining rotating machinery. Rolling elements bearings do not generate frequencies that are multiples of operating speed and unlike more basic faults, bearing faults appear in four stages. During stage one, bearings operate at normal conditions, and can be considered undamaged. At stage two, bearing defect frequencies begin to appear as peaks on the frequency spectrum. According to the article "Rolling Element Bearing Analysis" by Brian Graney and Ken Starry, bearing defect frequencies can be calculated using equations (3.1) through (3.4) [34]. The amplitudes of these frequencies hint toward the conditions of the bearing, and often increase over time. As the bearing deteriorates, it reaches stage three where multiples of the bearing defect frequencies begin to appear as peaks in the frequency spectrum. It is common practice to replace these bearings after reaching this stage. Finally, at stage four, bearing defect frequencies will be replaced by random noise in the frequencies between 2-5 KHz [35]. At this stage, the bearing is at the risk of undergoing catastrophic failure which can cost companies thousands in machine repair and/or replacement. By replacing damaged bearings before they fail, industries can drastically reduce the cost of replacing vital machinery therefore outlining the importance of predictive based maintenance on high value equipment.

The bearing defect frequencies were also calculated for the motor's 6203-2RS bearing. When the inner race of the bearing rotates the defect frequencies including ball pass frequency of the inner race and outer race (BPFI and BPFO), fundamental train frequency (FTF), and ball pass frequency (BPF) can be calculated using the following equations:

$$BPFI = \frac{N}{2} * F * (1 + \frac{B}{P} * cos\theta) \tag{3.1}$$

$$BPFO = \frac{N}{2} * F * (1 - \frac{B}{P} * cos\theta) \tag{3.2}$$

$$FTF = \frac{F}{2} * (1 - \frac{B}{P} * cos\theta) \tag{3.3}$$

$$BSF = \frac{P}{2B} * F * [1 - \left(\frac{B}{P} * cos\theta\right)^2] \tag{3.4}$$

Where N is number of bearing balls, F denotes shaft frequency (Hz), B represents ball diameter (mm), P is the pitch diameter (mm), and θ is the contact angle. The above fault frequencies can be approximately calculated using equations 3.5 through 3.8:

$$BPFO \cong 0.4 * N * F \tag{3.5}$$

$$BPFI \cong 0.6 * N * F \tag{3.6}$$

$$FTF \cong 0.4 * F \tag{3.7}$$

$$BSF \cong 0.2 * N * F \tag{3.8}$$

Using a bearing from a three phase induction motor, a defect was created on bearing cage. Figure 3.11 shows the generated defect on the motor's bearing.

Figure 3.11: The damaged bearing

Table 3.1 shows the calculated values for each bearing fault. The motor was operated at 30Hz. By doing this, it was predicted the bearing's corresponding frequency spectrum would exhibit traits correlating to one of four stages of bearing failure thus supporting the validity of using vibration analysis to conduct predictive based maintenance. The spectrum plots that have been used in this analysis is based on the algorithm proposed in [36] and [37].

Table 3.1: Bearing defect frequencies

Bearing Frequency Types	Frequency (Hz)
Shaft Speed Frequency	30
Inner race defect frequency (BPFI)	144
Outer race defect frequency (BPFO)	96
Fundamental Train Frequency (FTF)	12
Ball spin frequency (BSF)	48

Figure 3.12 displays the vibration data taken from the machine operating with the damaged bearing shown in figure 3.11. Same as previous situations, the vibration data is recorded using an accelerometer located on the radial axis of the motor.

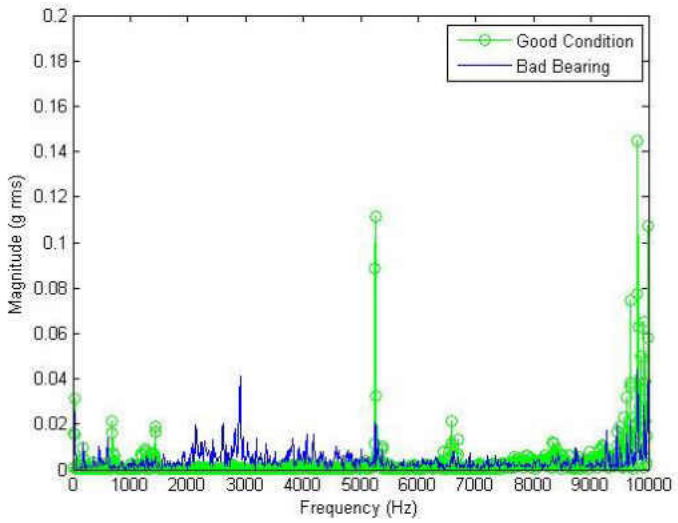

Figure 3.12: Vibration graph for damaged bearing condition.

Several notes can be taken from Figure 3.12. For instance, the vibration spectrum displays a raised noise floor as well as a number of low amplitude peaks appearing in the higher frequencies; however, what is interesting to note is that none of these frequencies appear to be whole number multiples of the running speed, or the bearing fault frequencies, yet it is obvious the motor's vibration data has been affected by the damaged bearing. Comparing these results to the healthy situation, shows how the motor's vibration data has undergone substantial change. The vibration data in frequency domain predicts stage four of bearing failure. Stage four of bearing failure displays large amounts of noise in higher frequencies. Should this be the case, depending on the significance of the motor's application, it is important to replace the bearing immediately. It is common practice to prevent machine bearings from reaching stage four of bearing failure,

otherwise the bearing is at the risk of experiencing catastrophic failure resulting in damage to vital machine components.

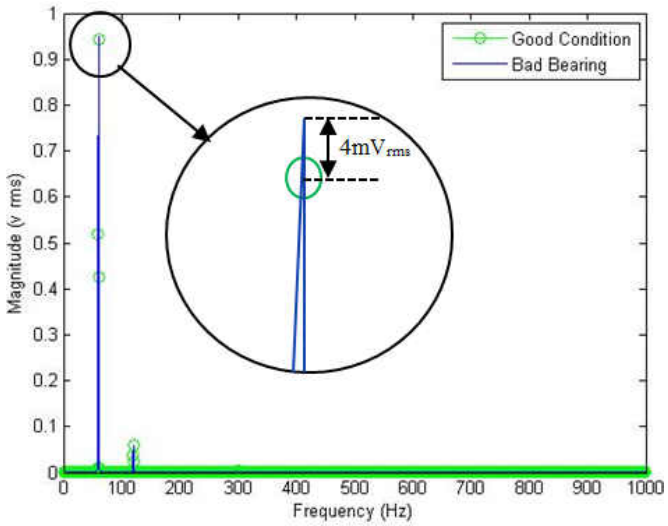

Figure 3.13: Current Graph for damaged bearing condition.

Figure 3.13 illustrates the frequency response of the stator's current. From the recorded data, it has been observed that the defected bearing will affect the stators current, slightly. Comparing current responses of unbalanced condition and damaged bearing situation, it is observed that the unbalanced load has affected the current response more than the damaged bearings.

3.3.4 Mechanical Looseness

Vibration patterns resulting from mechanical looseness were also studied. By loosening mounting bolts on the three phase electric motor, the body of the motor was allowed to move more freely therefore altering the motor's vibrational patterns. On the frequency spectrum, peaks corresponding with mechanical looseness are considered to

appear as several multiples of the motor's operating speed. Similar to previous experiment, the three phase motor's vibration data was operated at 30Hz.

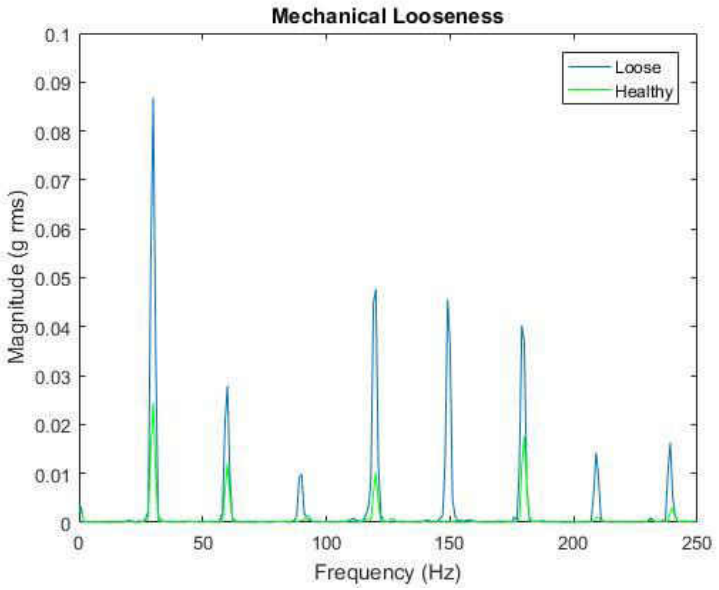

Figure 3.14: Vibration response due to mechanical looseness.

Figure 3.14 displays several peaks appearing in the low frequency spectrum. What is most notable of these peaks is that their frequency values are multiples of the running speed. Additionally, these peaks possess a variety of amplitudes each large enough to be considered hazardous to the motor's overall health. If allowed to operate over longer periods of time, it is likely the motor's lifespan will be reduced. Fortunately, mechanical looseness is often easy to address. In this case, simply tightening the bolts on the motor's mounting feet resolves the issue. These differences between the healthy condition and mechanical looseness prove that the presence of mechanical looseness condition appears as several multiples of the motor's running frequency as well as a raised noise floor in the spectrum and therefore agree with the conditions stated in [33].

3.3.5 Damaged Wires

When the motor is confronted to a high pulsed load torques and/or surge currents enforced from the AC drive, the stator wiring will be overloaded. This overload condition may increase the temperature of the wires. As a result, the resistance of the wires would increase. This increase will lead to a decrement in the current level of the defected phase of the motor, due to Ohm's law. Therefore, an unbalanced circulating electromagnetic filed will rotates around the rotor, which will increase the vibration generated in the machine.

Considering a three phase electric machines with main phase current variables symbolized as I_A, I_B and I_C; the motor current Vector components in stationary framework (I_D, I_Q) are as follows [17]:

$$i_D = (\sqrt{2}/\sqrt{3})\, i_A - (1/\sqrt{6})\, i_B - (1/\sqrt{6})\, i_C \tag{3.9}$$

$$i_Q = (1/\sqrt{2})\, i_B - (1/\sqrt{2})\, i_C \tag{3.10}$$

Under ideal conditions, the motor supply currents constitute a positive-sequence and the stationary vectors have the components described in (3.11) and (3.12).

$$i_D = \left(\frac{\sqrt{6}}{2}\right) i_+ \mathrm{Sin}(\omega t) \tag{3.11}$$

$$i_Q = (\sqrt{6}/2)\, i_+ \mathrm{Sin}(\omega \mathrm{t} - \tfrac{\pi}{2}) \tag{3.12}$$

Where i_+ is the maximum value of the current positive sequence (A), ω denotes the angular supply frequency (rad/s), and *t* denotes the time variable (s).

Under abnormal conditions, (3.11) and (3.12) are no longer valid, because the motor supply current will contain other components besides the positive-sequence component. In these conditions, the current D and Q vectors will contain a dominant harmonics, whose existence is directly related to the asymmetries either in the motor or in the voltage supply system [38]. The aforementioned asymmetry in the motor's current components will result in excessive vibration in the motor.

Figure 3.15 shows the effect of bad wiring on the vibration of the motor. In this condition, the motors vibration is slightly increased as compared to normal condition. In other words, as the increased resistance would decrease the magnetic motive force (MMF) in one of the wires, this would act like an unbalanced load torque. However, the vibration spectrum shown in

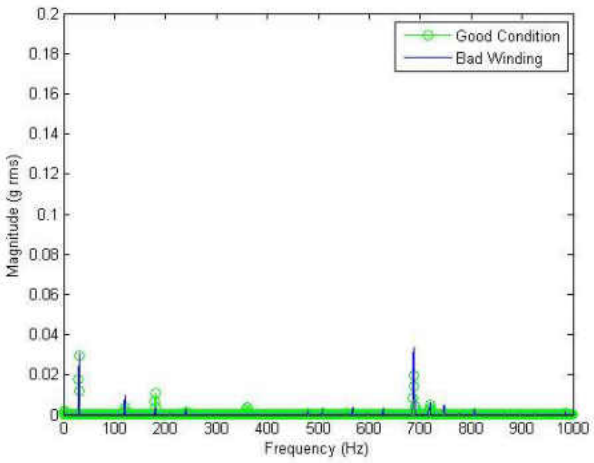

Figure 3.15: Machine's vibration response to damaged stator's windings condition.

Figure 3.15 depicts a very minor increase in the vibration's amplitude at the operating speed which is very insignificant compared to other faults such as unbalanced condition. Figure 3.16 displays the electric current response of the damaged windings.

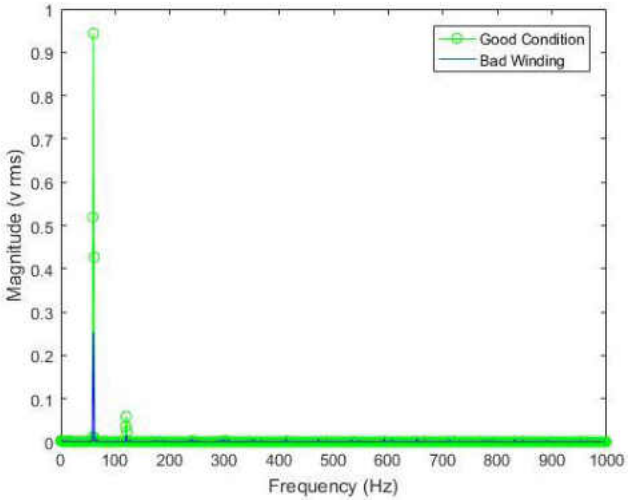

Figure 3.16: Electric current response of the damaged windings

Figure 3.16 shows how the damaged windings have affected the current response of the motor. The increased resistance of the wires would result in the current drop due to ohm's law. This faulty condition has not merely changed the vibration response of the machine which is due to the closed loop control system within the AC drive. The drive would modify the current for other windings which would result in a balanced situation. The damaged windings affect the protection system within the drive and would result in machine's complete shutdown. This experiment proves that the best monitoring method is a combination of the available monitoring techniques.

3.3.6 Shaft Misalignment

In this section, using the machinery fault simulator a shaft misalignment condition is investigated. The healthy condition of the machinery fault simulator has similar vibration response as the 3 phase induction machine of setup number one.

Good shaft alignment practice is a vital step in maintenance procedure of rotating machines. Some symptoms of a misaligned shaft are [39]: loose or broken foundation bolts, oil leakage at bearing seals, loose or broken coupling bolts, shafts breaking or cracking, and increased temperature on different components of the machine such as bearings or couplings. In this experiment, in order to stimulate the parallel misalignment, the shaft was moved 20 mils and the vibration data from one end of shaft is measured.

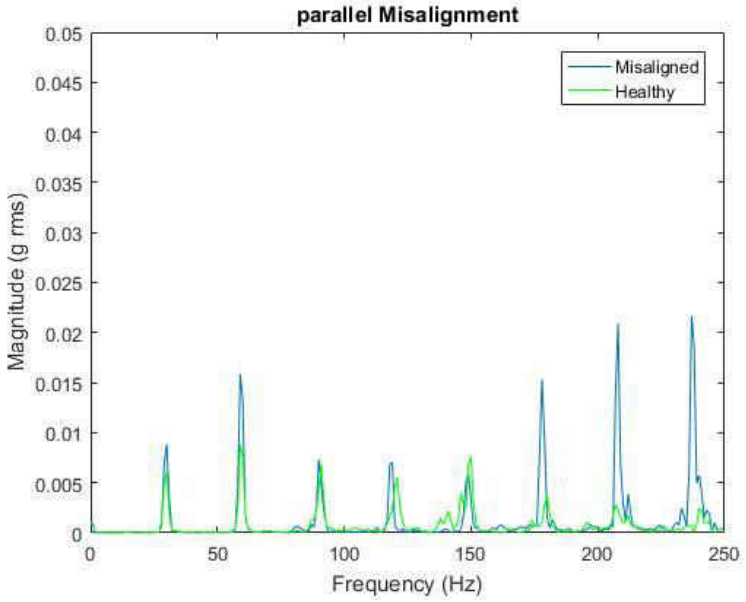

Figure 3.17: Vibration response of the misaligned shaft.

Figure 3.17 displays the vibration response of the misaligned shaft. The case of parallel misalignment is very noteworthy; in this case the vibration's amplitude at the operating speed has increased mildly and the 2X operating speed is showing larger amplitudes. As a matter of fact, these harmonics are known as the characteristic frequency responses corresponding to the parallel misalignment condition. Moreover, it's noteworthy that the amplitudes at 6, 7, and 8X operating speed have also increased significantly for the misaligned condition.

3.4 Chapter Summary

The results from each of the tests support the use of vibration analysis in predictive based maintenance. By comparing the vibration data for each failure case to the healthy condition, the patterns corresponding with each fault condition are outlined. This shows how certain faults in rotating mechanical systems can be determined using vibration analysis. Additionally, vibration analysis can also determine the severity of these faults and help engineers predict when machinery will fail. Identifying these faults can help companies reduce the cost of maintenance and repair of high value machinery. The electric current was also measured to investigate the effects of damaged winding on the vibration response of the machine. Moreover, the current signal was also investigated while mechanical faults such as damaged bearing or unbalanced rotor are present. The result proves that the current data does identify the present fault; however, it cannot categorize the type of failure precisely.

CHAPTER 4

FAULT CORRECTION

4.1 Overview

In this chapter, correction methods for different faults studied in chapter 3, are investigated. The main content of this chapter inspects the unbalanced rotor. The vibrations due to unbalanced situation can be controlled by adding a correction mass to the flywheel. However, the location where this mass is added to has the most significant effect on the vibrations of the machine. For this purpose, a novel approach which uses image processing methods to find the corresponding location of the correction mass is developed.

4.2 Balancing Technique

Here, a novel computer vision approach developed for balancing of rotating machines is discussed. Different methodologies are investigated to stabilize the unbalanced rotor. First, a method is discussed which will eliminate the need for the balancing equipment, and the exact location of the balancing mass is identified using solely the accelerometer data and intricate vibration theories. Considering a rotor supported on two bearings, the trial masses can be added to each of the two planes on

each side of this rotor which are called planes A and B. The governing equations to find the trial mass are:

$$\varphi_A = \tan^{-1}\left[\frac{\left(A_1^{90}\right)^2-(\Delta A_1)^2-A^2}{\left(A_1^{0}\right)^2-(\Delta A_1)^2-A^2}\right] \tag{4.1}$$

$$\Delta A_1 = \sqrt{\frac{\left(A_1^{0}\right)^2+\left(A_1^{180}\right)^2-2A^2}{2}} \tag{4.2}$$

$$\Delta A_2 = \sqrt{\frac{\left(A_2^{0}\right)^2+\left(A_2^{180}\right)^2-2A^2}{2}} \tag{4.3}$$

$$\varphi_B = \tan^{-1}\left[\frac{\left(B_1^{90}\right)^2-(\Delta B_1)^2-B^2}{\left(B_1^{0}\right)^2-(\Delta B_1)^2-B^2}\right] \tag{4.4}$$

$$\Delta B_1 = \sqrt{\frac{\left(B_1^{0}\right)^2+\left(B_1^{180}\right)^2-2B^2}{2}} \tag{4.5}$$

$$\Delta B_2 = \sqrt{\frac{\left(B_2^{0}\right)^2+\left(B_2^{180}\right)^2-2B^2}{2}} \tag{4.6}$$

Where A represents the vibration magnitude on bearing A for the unbalanced rotor, φ_A is the phase angle on bearing A for the unbalanced rotor, ΔA_1 is the additional vibration magnitude when the trial mass is added to plane A, ΔA_2 is the additional vibration magnitude when the trial mass is added to plane B [40].

Similarly, B, φ_B, ΔB_1, ΔB_2 are defined. The correction factors which define the location of the mass are defined by the following equations:

$$R_{AX}\Delta A_1 + R_{BX}\Delta A_2 = -A\cos\varphi_A \tag{4.7}$$

$$R_{AX}\Delta B_1 + R_{BX}\Delta B_2 = -B\cos\varphi_B \tag{4.8}$$

$$R_{AY}\Delta A_1 + R_{BY}\Delta A_2 = -A\sin\varphi_A \tag{4.9}$$

$$R_{AY}\Delta B_1 + R_{BY}\Delta B_2 = -B\sin\varphi_B \tag{4.10}$$

The required balancing mass is the product of correction factors and the trial mass. The proposed method provides accurate results. However, it requires 8 different measurements while a trial mass is added to four different angles on each of the two planes of the rotor. Therefore, it requires taking more intricate measurements and while there is a lack of accessibility to the rotor, this method cannot be implemented. In the methodology developed, the phase angle is measured based on combination of the accelerometer data along with a video recording of the rotating flywheel. This method only requires two measurements, one from the original unbalanced condition, another one after adding a trial mass to a marked location on the rotor. The rotor is being recorded during this process. The goal is to identify the position of the marked area whenever the amplitude of the sinusoidal vibration response reaches the maximum.

In this experiment the motor is set to run at 20 Hz (1200 RPM), the operating speed can be set lower to ease detecting features on the marker. Results achieved at lower speeds can be verified at higher operating speeds. It is important to find a speed to make sure the features detected have high intensity values that can be used for a proper edge and line detection scheme. In this experiment for capturing the video of the rotating shaft the IPhone 6 camera is used in slow motion mode which results in capturing 240 frames per second.

4.3 Edge Detection

Edge detection is a tool for finding boundaries of the objects in an image. These boundaries at which the image brightness changes significantly are identified as edges. There are multiple edge detection methods available such as Sobel, Roberts and Canny edge detectors. Canny edge detector is the most efficient edge detector [41]. Here, different edge detectors are investigated to find the best edge detection method. Sobel edge detectors use the following 3X3 kernels which are used to convolve the image and calculate the horizontal and vertical changes [42].

$$G_x = \begin{bmatrix} -1 & 0 & 1 \\ -2 & 0 & 2 \\ -1 & 0 & 1 \end{bmatrix}, G_y = \begin{bmatrix} -1 & -2 & -1 \\ 0 & 0 & 0 \\ 1 & 2 & 1 \end{bmatrix} \tag{4.11}$$

$$G = \sqrt{{G_x}^2 + {G_y}^2} \tag{4.12}$$

$$\theta = \text{atan}(\frac{G_y}{G_x}) \tag{4.13}$$

Where G_x is the horizontal kernel, G_y is the vertical kernel, G is the gradient magnitude, and θ is the gradient's direction. The areas which have high gradients are identified as edges. Roberts edge detectors use the following two kernels [43]:

$$G_x = \begin{bmatrix} 1 & 0 \\ 0 & -1 \end{bmatrix}, G_y = \begin{bmatrix} 0 & 1 \\ -1 & 0 \end{bmatrix} \tag{4.14}$$

The Canny edge detector use the following process: First a Gaussian filter is implemented to smooth the image. Then it finds the intensity gradients of the image and applies a non-maximal suppression. Next it defines specific thresholds automatically to determine the edges and tracks them using hysteresis [41]; it is possible to modify the

threshold but was not necessary as the results were satisfactory for line detection. The edge detection procedures are available as MATLAB functions. The results of implementing different edge detectors are demonstrated in figure 4.1.

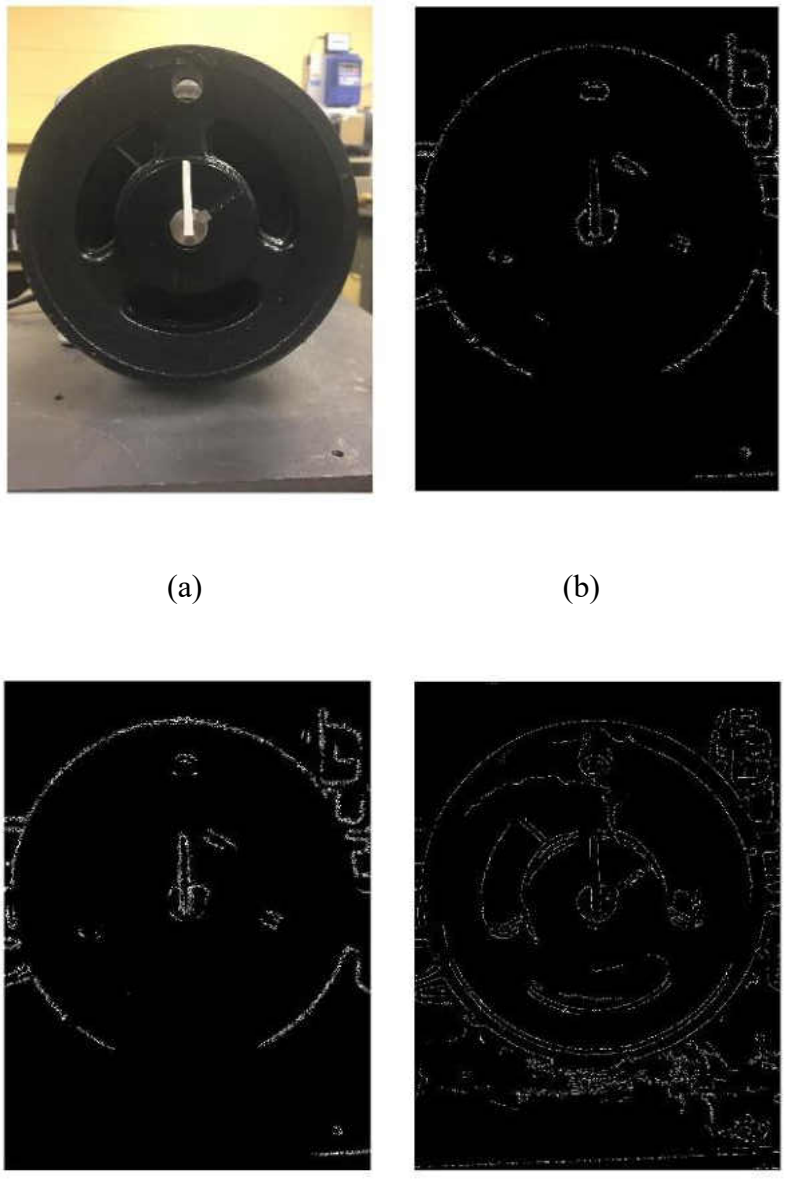

(a) (b)

(c) (d)

Figure 4.1: Edge detection methods. (a) Original image, (b) Sobel edges, (c) Roberts edges, (d) Canny edges.

From figure 4.1, it is shown that Canny edge detectors (d) have detected more edges compared to Sobel (b) or Roberts (c) edge detectors. This is verified visually and numerically based on their histograms, which verifies that the Canny edge detectors have identified more white pixels. On a 2448*3264 pixels image Canny has identified 385250 white pixels compared to 61878 and 65687 white pixels for Sobel and Roberts respectively.

4.4 Line Detection

In order to detect the location of the marker on the flywheel, a line detection algorithm is implemented. RANSAC and Hough transform [44] are the most common line detection algorithms available. Here, Hough transform is implemented to detect the marker line and subsequently the slope of this line is identified for an automatic balancing scheme. Note that to achieve the perfect line detection algorithm the thresholds for Hough peaks are considered low. The threshold is modified to show one single line on the marker and avoid the unnecessary noises. Moreover, an algorithm can be developed to refit lines based on based on strength of the Hough peaks. More importantly, in this study the effects of camera distortion were not considered effective on the final results. However, for more precision, it is recommended to calibrate the camera, and undistort the images based on camera parameters [45].

Figure 4.2 displays the marker lines detected on the image taken from the flywheel. Later on, the lines will be detected on the frames of the captured video of rotating flywheel.

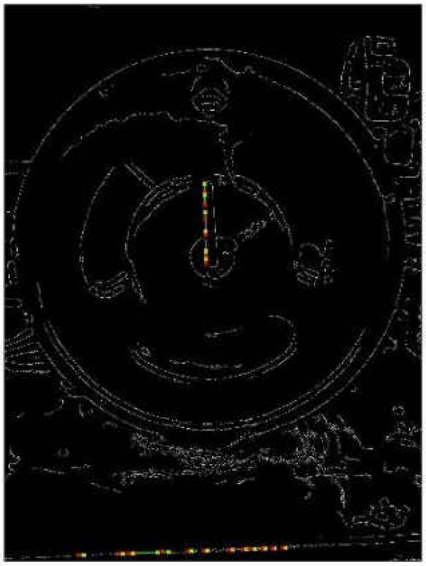

Figure 4.2: The Hough lines detected on the marker.

Figure 4.2 displays the Hough line detected on the marker. The corresponding phase angle here is 0 degrees, which is considered as a reference point (It will be called 12 o'clock as a reference position). As mentioned earlier the video is recorded from camera on slow motion mode which can grab 240 frames per second. When motor is operating at 20 Hz (1200 RPM) 20 peaks in the vibration spectrum are observed per second that means for each one full rotation of the flywheel, 12 frames will be recorded. If more accuracy is desired, the operating speed of the motor could be reduced or a more advanced camera should be used.

4.5 Machine Vision Based Balancing Method

Vibration response of the healthy system is measured in radial axis. Next an external mass is added to the flywheel to stimulate the unbalanced rotor situation. Figures 4.3 and 4.4 display the vibration response of the healthy and unbalanced conditions in time domain.

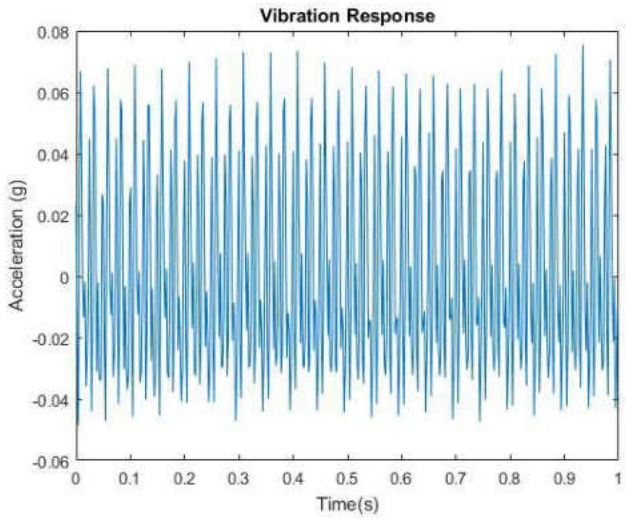

Figure 4.3: Vibration response of the healthy condition in time domain.

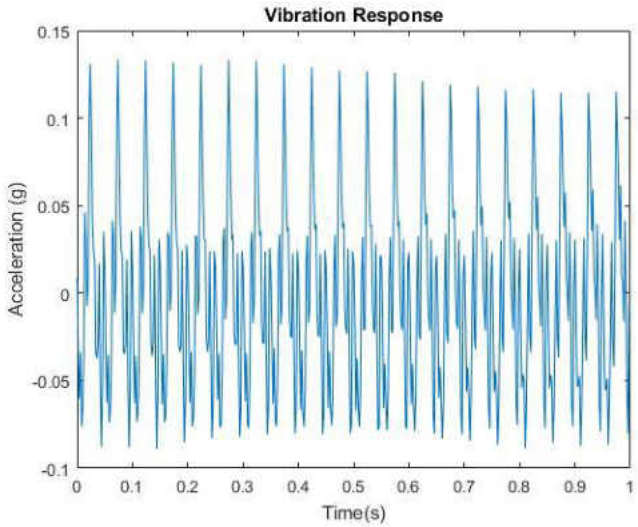

Figure 4.4: Vibration response of unbalanced condition in time domain.

Comparing figures 4.3 and 4.4, it is clear that by adding the external mass the overall vibrations of the system has increased significantly (as mentioned in chapter 3), because the machine is affected by an increased force of:

$$F = m * e * \omega^2 \tag{4.15}$$

Where F represents the unbalanced force, m is the unbalanced mass, e represents the distance from the unbalanced mass to the center of rotation, and ω is the operating speed of the machine.

The recorded video and the vibration response in time domain are investigated together to determine the position of the marker when the sinusoidal vibration response reaches maximum. It is clear that the marker stays at the same spot when the vibration amplitudes reach the next maxima. The marker location is shown in figure 4.5.

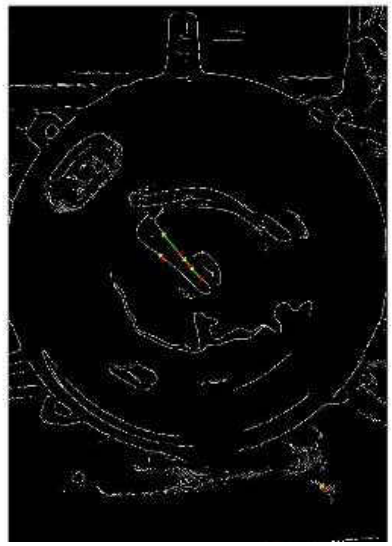

Figure 4.5: Phase angle of the unbalanced flywheel.

Figure 4.5 shows that the Hough line is pointing toward 11 o'clock meaning the phase angle is about 30 degrees. The maximum amplitude of the vibrations in this situation derived from figure 4.4 is 0.133 g. Moreover, when other lines are detected in the image, a weighted average of the most significant lines is used to avoid the pointless lines detected around the region of interest.

Next, a trial mass weighing 63.6 gram is added to a random location on the flywheel as seen of figure 4.6.

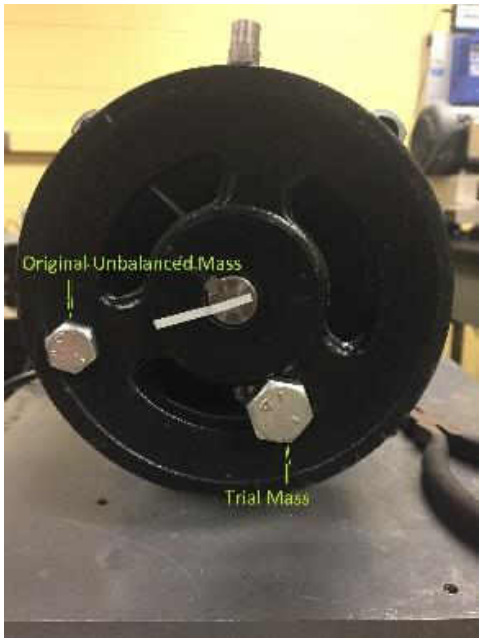

Figure 4.6: A trial mass added on the flywheel.

The vibration data and the video is recorded for the second time. The vibration data is shown in figure 4.7.

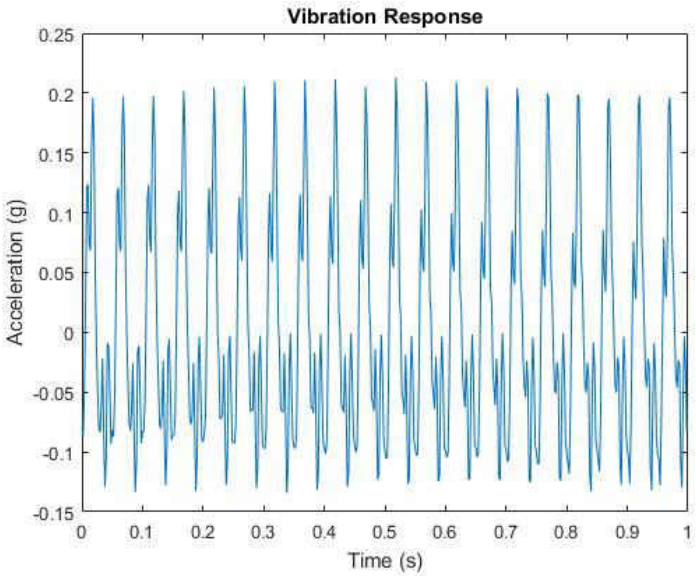

Figure 4.7: Vibration response of the system when a trial mass is added.

Figure 4.7 shows that the maximum vibration when a trial mass is added to the unbalanced rotor is 0.213 g which is identified using MATLAB. As seen on figure 4.8, the phase angle is measured as 120 degrees (line pointing toward 8 o'clock).

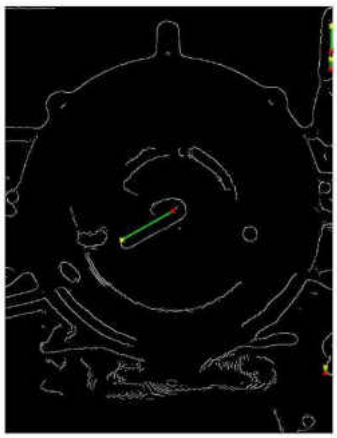

Figure 4.8: Phase angle when the trial mass is added.

Based on the values derived from the videos and accelerometer data, two vectors are identified. $\vec{a}$ is defined by maximum vibrations amplitude value and phase angle of the

original unbalanced flywheel. $\vec{b}$ is defined by maximum vibrations amplitude and phase angle of the flywheel after the trial mass is added to it. Figure 4.9 demonstrates the vectors on the polar coordinates.

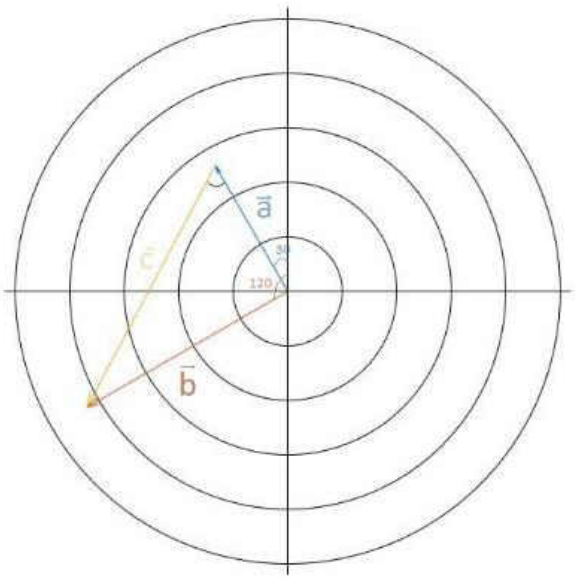

Figure 4.9: The orientation vectors on polar coordinates.

In figure 4.9, $\vec{c}$ is defined as:

$$\vec{c} = \vec{b} - \vec{a} \tag{4.16}$$

Here the objective is to find the amount of angle φ which is the angle shown between $\vec{a}$ and $\vec{c}$ and it denotes how much the trial mass has to be rotated with respect to the center. Based on the values measured, with simple math based vector analysis, adjustment angle of φ is calculated 58 degrees. While the accuracy was identified in 30 degrees increments, φ value is considered 60 degrees. Therefore, the trial mass is rotated 60 degrees and the following vibration response shown in figure 4.10 is achieved.

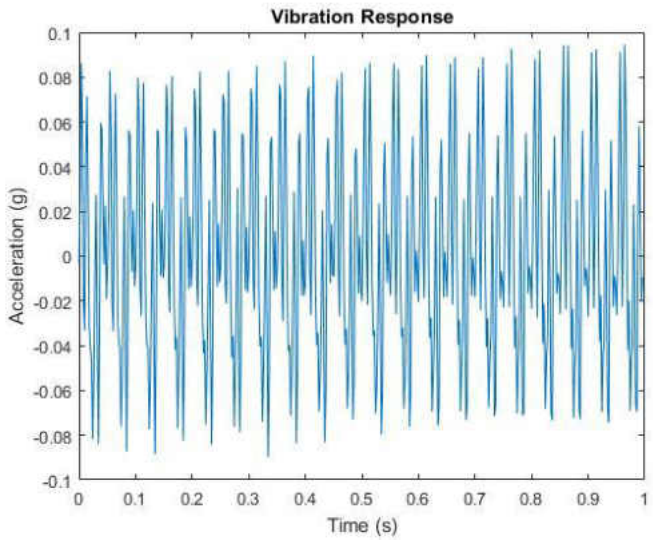

Figure 4.10: The balanced flywheel vibration response.

Figure 4.10 demonstrates the vibration response of the system when the trial mass is added to the correct location on the unbalanced flywheel. Notice that the vibrations amplitude has decreased compared to both previous unbalanced situations. Figure 4.11 shows the frequency response of all investigated conditions using FFT in linear form.

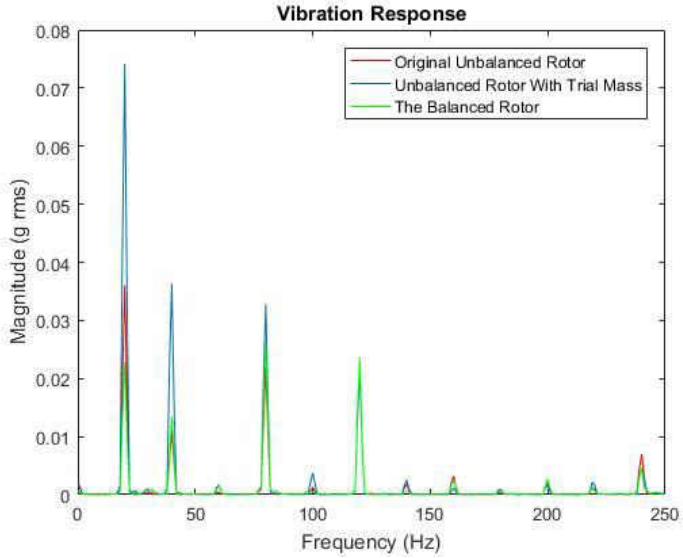

Figure 4.11: The frequency response of the investigated conditions.

Figure 4.11 confirms how the vibrations of the system have reduced significantly after it was stabilized by adding the trial mass to the correct location on the flywheel. This system can become completely balanced when the correct mass of M derived from equation (4.17) is added to the determined location.

$$M = \frac{|\vec{a}|}{|\vec{c}|} * m_{trial} \tag{4.17}$$

$$M = \frac{0.133}{0.2511} * 63.6 = 33.68\ grams \tag{4.18}$$

Therefore, the adjusted trial mass of 33.68 grams would have resulted in making the rotor completely balanced. It is important to note that the original unbalanced mass was 30.77 grams, 2.91 grams difference (%9.45) from the calculated value.

4.6 Different Faults Correction

In rotating machine's failure correction, the unbalanced situation is provided with a correction method that does not necessarily require to remove and replace the rotating components. However, other methods are not improvised as simple as the unbalanced situation. When the characteristic frequency of the machine points toward mechanical looseness, the only approach is to recover machine's health situation by connecting it sturdier to its base. This process does not always require machine's stoppage and could be achieved instantaneously.

When damaged wires are identified, the machine has to be shut down immediately and the stator's wires have to be replaced. Bearing faults correction is more interesting, when the bearing failure frequencies such as BPFO, BPFI, and etc. are identified, the

machine is not stopped; however, it's more frequently monitored to identify the faults development patterns. The moment the random noise at frequencies between 2-5 KHz appears. The machine's operation has to be stopped and the bearings must be replaced.

A misaligned shaft puts strain on the rotating machine and can damage the bearings, couplings, mounting bolts and other machine components. Therefore, the manufacturing companies have identified maximum allowable tolerances of misalignment for the machines based on their operating speed, this tolerance simply decreases by higher operating speeds. For correcting misalignment, the shafts have to be aligned in both vertical and horizontal planes. For shaft alignment the dial gauges are used as shown in figure 4.12.

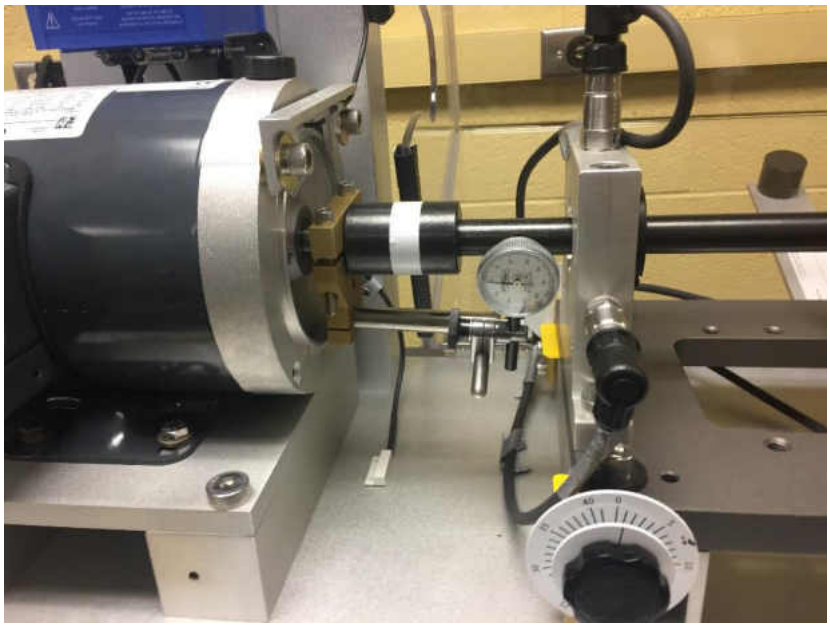

Figure 4.12: Shaft alignment gauge attached to the shafts.

Based on total indicator readings (TIR), the dial gauge is set to zero at a specific location such as the one shown on figure 4.12, and then roll it 180 degrees and read the

gauge value. The actual offset of the shaft is half of the value shown on the dial gauge. Another method is to use validity rule which the readings on the gauge are taken at 90 degree intervals. The validity rule says the sum of the values recorded on top and bottom is equal to the sum of the values taken from the sides. This helps when there exists lack of accessibility to one side; in other words, the third value can be calculated based on the other three. Therefore, when the amount of misalignment is measured the shaft will be moved on the two planes to achieve a completely collinear system.

4.7 Chapter Summary

In this chapter the correction methods for the common rotating machine's faults are studied. The main content of this chapter was to develop a method for reducing vibrations due to unbalanced condition. A method was developed which uses the accelerometer data combined with a video taken from the machine to identify the amount of correction mass and its corresponding location on the flywheel. This method reduces the need for using advanced equipment, and does not require taking so many measurements from the machine. Basically, this method is developed to create a smartphone application. The reliability of the application is depending on the quality of the camera and sensitivity of mobile phone's accelerometers.

The correction methods for other types of failures such as damaged bearings and stator's wires, and misalignment are also briefly discussed.

CHAPTER 5

STATISTICAL ANALYSIS OF VIBRATION DATA

5.1 Overview

In this chapter different statistical methods are investigated to find and categorize the present faults in the system. These statistical methods include Principal Components Analysis (PCA), K-Nearest Neighbor (KNN), and Singular Value Decomposition (SVD). The methods implemented have categorized system failures based on their signature responses and severities.

5.2 Principal Components Analysis

Due to substantial improvements in computer processing, the concept of autonomous pattern recognition has become more effective. One of these processes is known as principal component analysis (PCA). This process would reduce the training needed by analyst and hopefully increase the accuracy of predictive maintenance. Rather than analyze vibration data manually, PCA can be used computationally to find the patterns associated with mechanical faults. For example, one misaligned motor can be grouped with other motors that share the same fault condition. The same principal applies for other types of mechanical faults. This notion points towards the automation of the

vibration analysis process which, in turn, will reduce a large portion of the costs associated with the maintenance industry. For this reason, an experiment was conducted to apply PCA towards fault detection and determine if this method could be deemed both efficient and reliable enough to merit further study and perhaps see an application within an industrial setting.

Principal component analysis is a statistical approach for separating large amounts of data with multiple variables. In other words, PCA is a feature extraction technique capable of distinguishing data values based on their respective variance to the rest of the data set [46]. This is done by calculating the amount of variance between several data sets and assigning each variable its own dimension to determine which variables have the largest impact on variance within the data [47]. By doing this, data of different types are separated into "groups" which can then be recognized by identifying one data set within that group. This is commonly used to find patterns in statistical information as seen in [48], which explains the application of PCA to organize a large number of cells into groups based on the genes they possess. The mathematical equation to derive the principal components is described in [49].

Fault detection, in its nature, involves the identification of vibration patterns. This section explores how PCA could be applied to determine these patterns computationally without the need of manual data analysis. By comparing large numbers of data sets, PCA can be used to group known vibration patterns based on their relevant trends. At which point, unknown data can be introduced so it can be grouped into their respective fault categories. This provides a new method of maintenance within industrial applications and could stand as the foundation for future research regarding this application.

For any operating condition of a motor, a change in spectral patterns can be observed in the frequency response when a system experiences varying degrees of fault severity. To account for the variance in vibration data in the PCA method, fault severity was altered for every test. Since a healthy motor cannot experience different degrees of healthiness, additional load was added to the motor under healthy conditions in order to change the response of the spectral pattern, thus simulating changing circumstances. Although load does not directly create a larger fault severity, for the purpose of this experiment it was assumed that an increased severity or load would intensify the response in the vibration data.

These tests involved three operating conditions of a typical axle system connected to an induction motor. The axle itself was under load supported by two bearing couples whose respective vibration data was recorded using a set of accelerometers mounted at several locations. Resultant FFT data was processed using PCA which helped outline any patterns that emerged from the experimental data. The validity of these patterns were tested using several unknown data sets to determine if they could be identified correctly.

For the series of healthy system tests, washers were added uniformly around the rotor to increase the amount of load applied to the system. This was done in multiples of four, starting zero and going until there were a total of 20. Unbalanced tests were conducted by adding washers in sets of two, starting at zero and going to 20. Figure 5.1 shows the rotor used to add load and simulate unbalance.

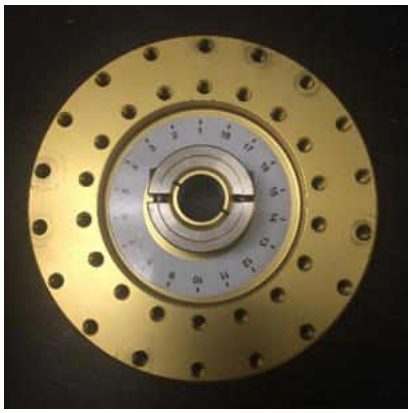

Figure 5.1: The flywheel used to simulate unbalance.

Misalignment was simulated via the misalignment dial in place on the MFS as seen on figure 5.2. These tests increased by five milli-inches (mils) starting at 10 mils and ending at 35 mils.

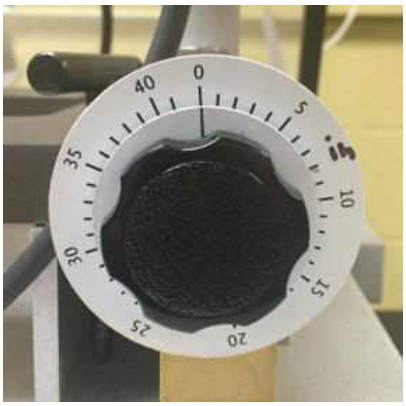

Figure 5.2: Dial used for introducing misalignment.

By changing the severity of the faults and the load of the healthy condition, the robustness of the PCA method was tested. This was done to determine if PCA could correctly group faults of the same type together that had different operating conditions. This is the main reason other failure types were not investigated in this study. It was not

possible to define different bearing fault severities and damaged wirings had little effect on the vibration data.

As mentioned earlier, the operating conditions of the motor tested were healthy, misalignment, and rotor unbalance. The healthy data set was taken to act as a control group for the other test sets. The fault conditions studied were tested to determine if the PCA method could correctly group the operating conditions by type and identify fault severity. With that said, the severity of one fault compared with another, was not investigated in this study. Instead, the intention of this experiment was to evaluate the trend of each fault group individually. For example, the most severe instance of misalignment cannot be compared with the most severe instance of unbalanced because the systems were operating under different conditions. Rather, it was intended that for each fault, a trend in fault severity would emerge. This would allow for an unknown test set to have the severity of its fault estimated.

A series of unknown vibration data were investigated to demonstrate the robustness of this statistical method. The unknown healthy test was taken with nine washers arranged uniformly the rotor. The unknown unbalanced test was taken with seven washers. The unknown misalignment test was conducted at 27 mils. Because each recorded test was controlled, the location of unknown tests could be compared to that of each known test by creating a region in which the fault was known. By doing this, unknown tests could be identified by determining if the test lied within the proximity of the region specific to that fault condition.

The vibration data is recorded on four accelerometers two of which are mounted on each bearing housings radially. The processed data sets for each accelerometer are

represented in figures 5.3-5.6. Each data set displays both the scores (red) and loadings plot of the PCA. In short, the square plot is represented by a large number of points each of which represents a single frequency value in the graph. On the other hand, the points representing the loadings portion of the graph are each a single test (unbalance, healthy, etc.). Additionally, each point in the loadings portion of the graph are marked with either an “h” (healthy), a “u” (unbalanced), or an “m” (misalignment) as well as the test number for that fault type in order of occurrence.

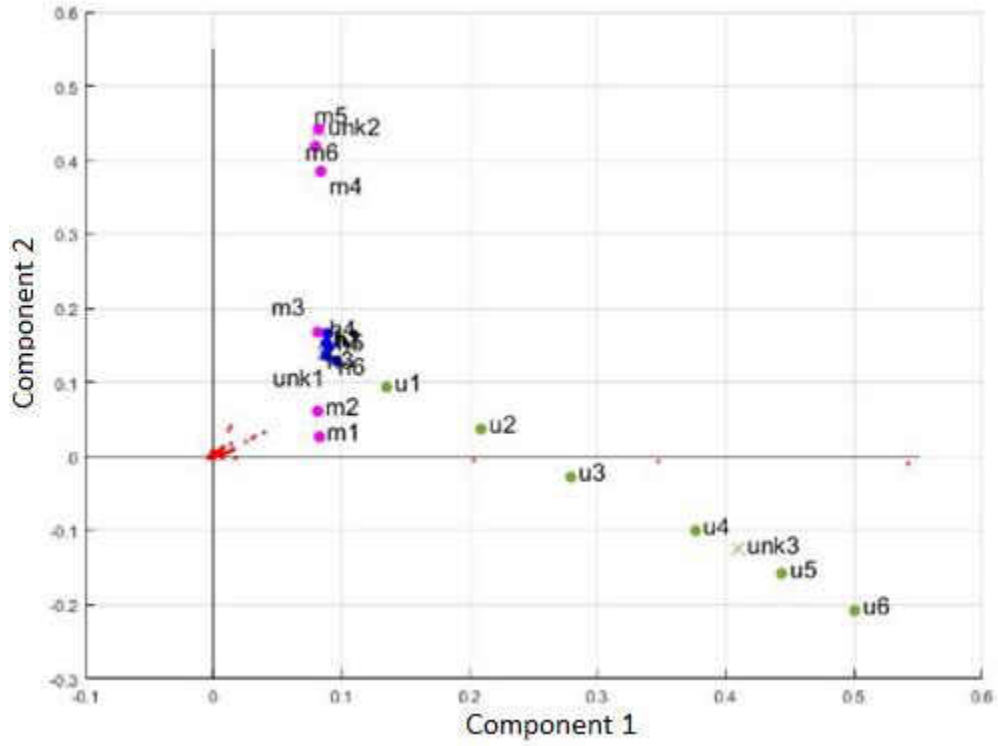

Figure 5.3: Accelerometer 1 PCA.

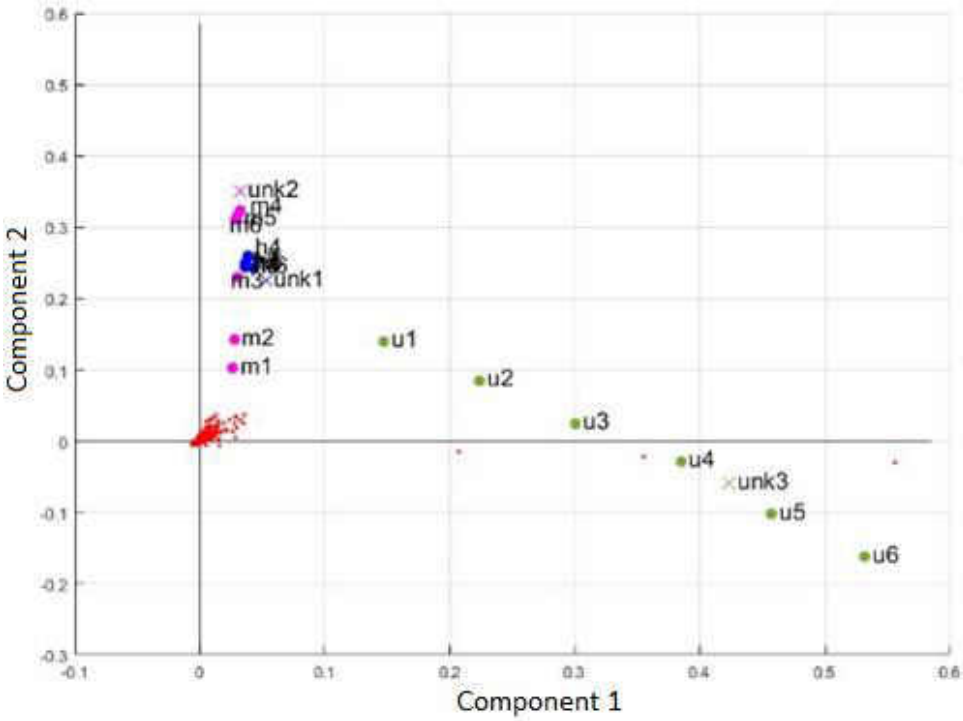

Figure 5.4: Accelerometer 2 PCA.

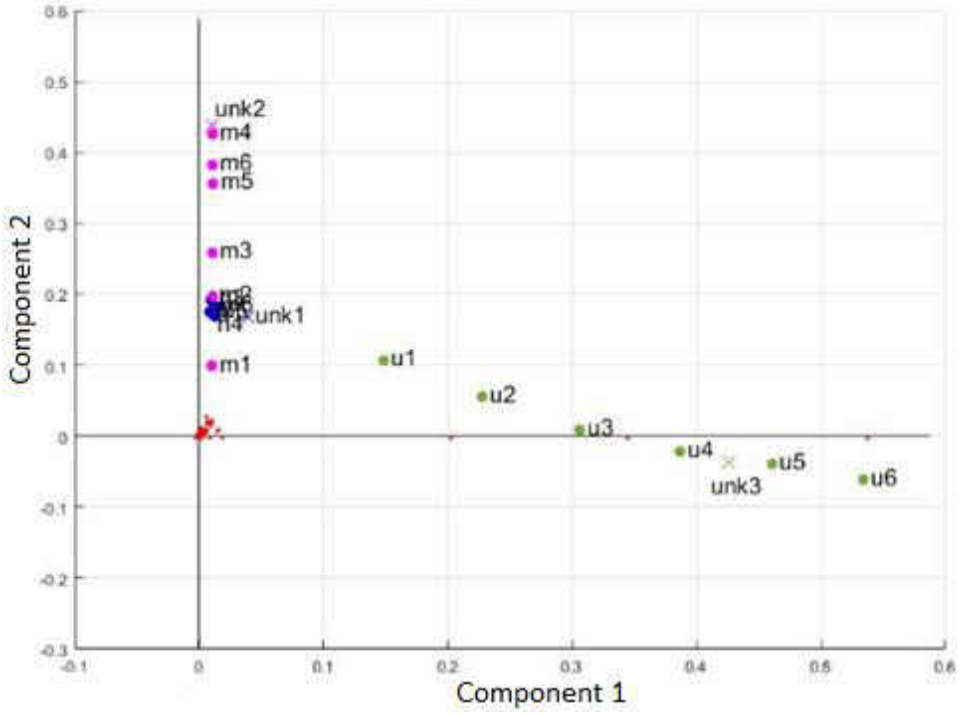

Figure 5.5: Accelerometer 3 PCA.

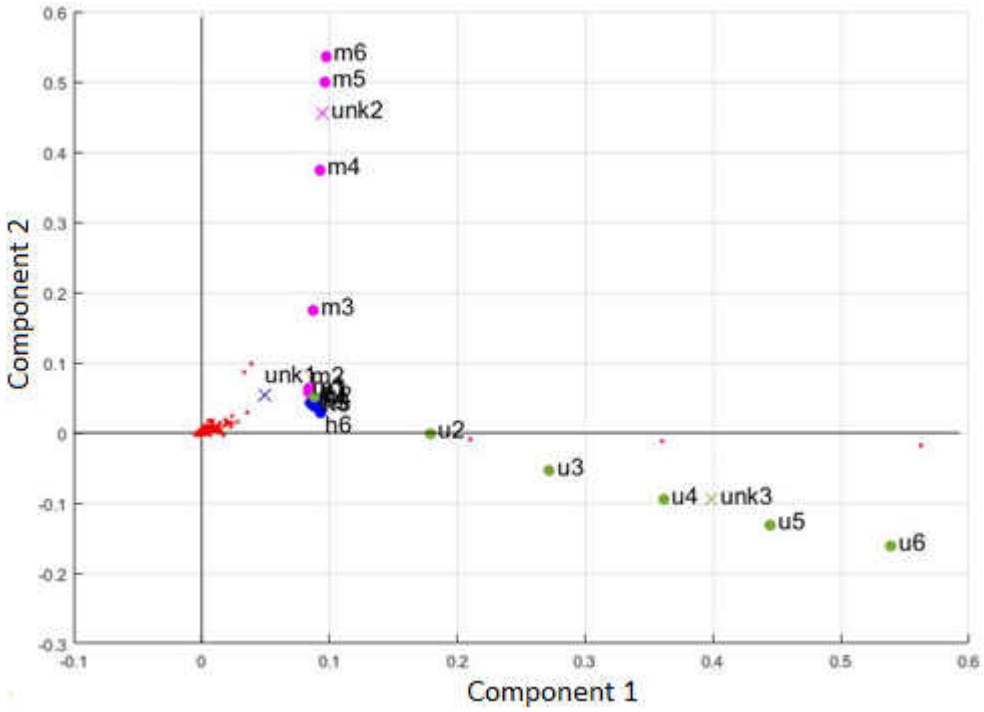

Figure 5.6: Accelerometer 4 PCA.

Figures 5.3-5.6 demonstrate how the mechanical faults have been categorized with respect to their corresponding vibration signature. It was expected that the healthy situations will not have too much variance and therefore, they have been located very close to each other. The unbalanced situation has a direct relation to the amount of unbalanced mass added to the rotating flywheel and therefore, a pattern based on failure severity is recognized within all accelerometers data. This trend is not recognized with the misaligned shaft as all the corresponding characteristic frequencies do not have a direct relationship with the amount of misalignment. It is clear from the figures that the unknown vibration data was in fact determined correctly.

The data shown on figures 5.3-5.6 are based on the first two components. It is seen on the figures that the region around the healthy condition is noisy and separating the

faulty and healthy conditions are not precisely possible. Therefore, the third component is taken into consideration. Figures 5.7 through 5.10 represent the same data presented in the previous section of this report. The only difference is that a third principal component is added thus adding another dimension of reference to the graphs. Besides this however, the data is presented in the same manner with both the loadings and score plot displayed in each figure.

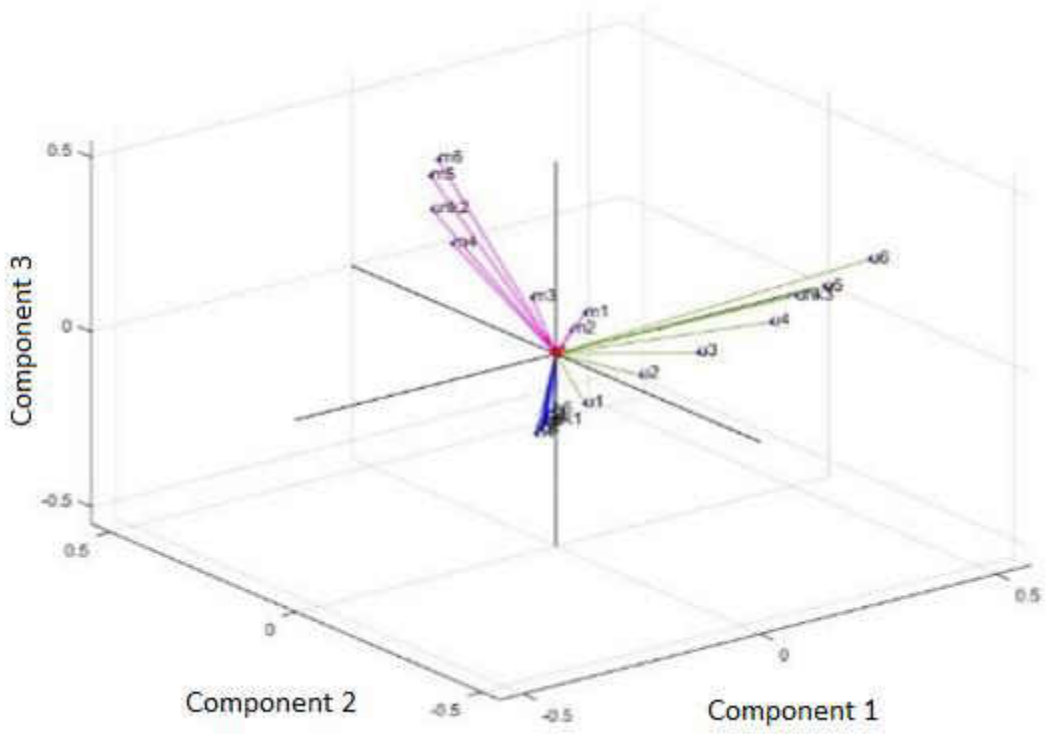

Figure 5.7: Accelerometer 1, 3 dimensional PCA.

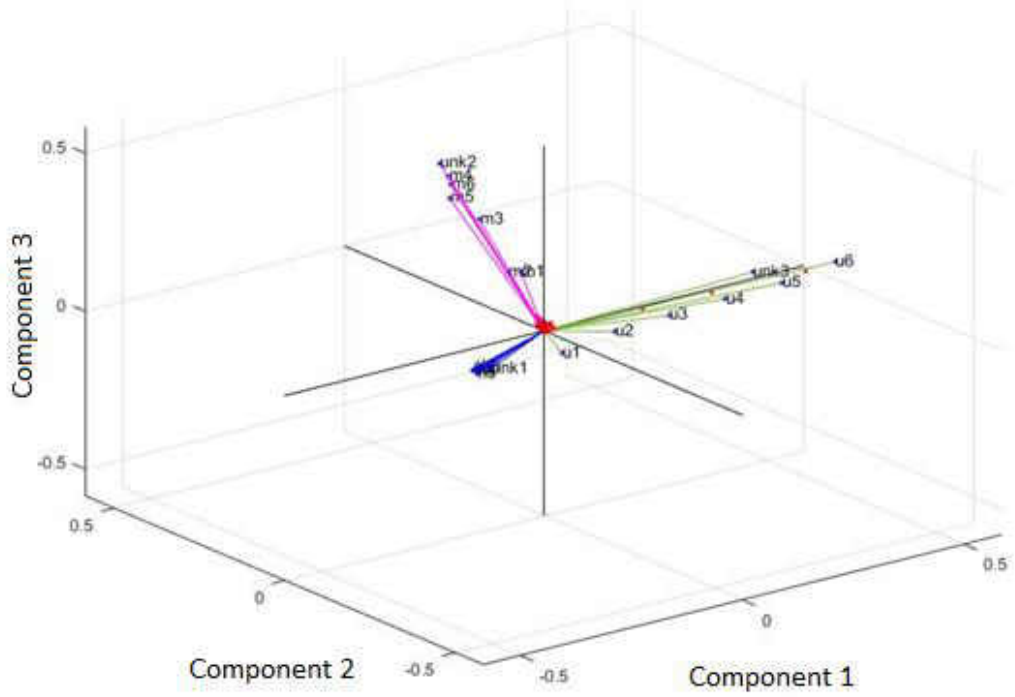

Figure 5.8: Accelerometer 2, 3 dimensional PCA.

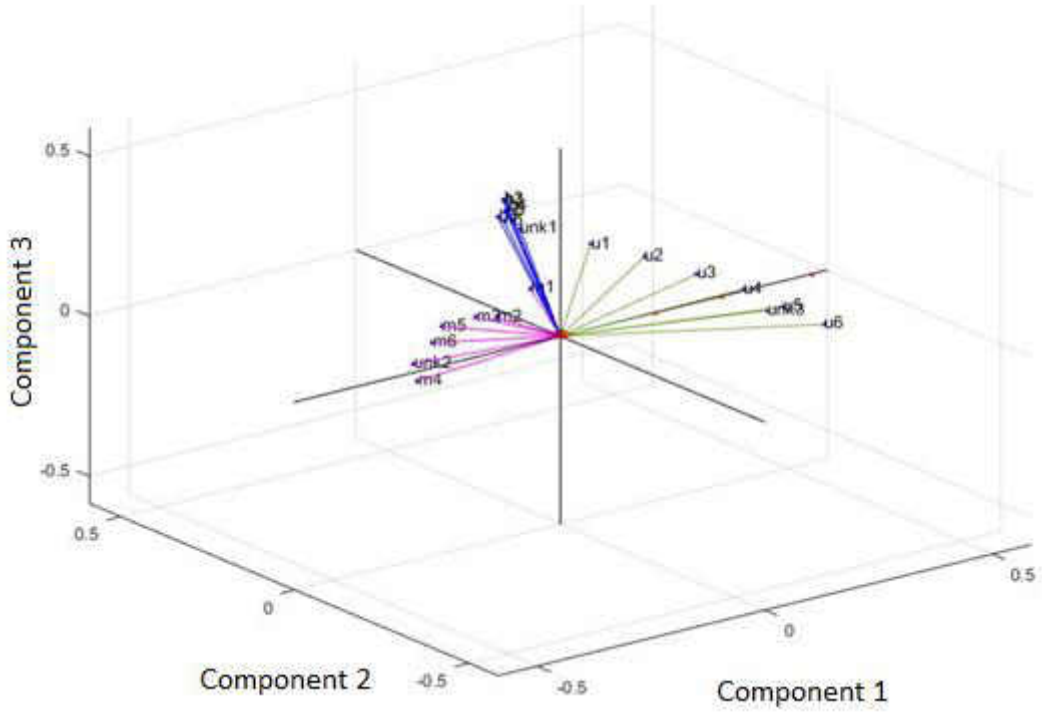

Figure 5.9: Accelerometer 3, 3 dimensional PCA.

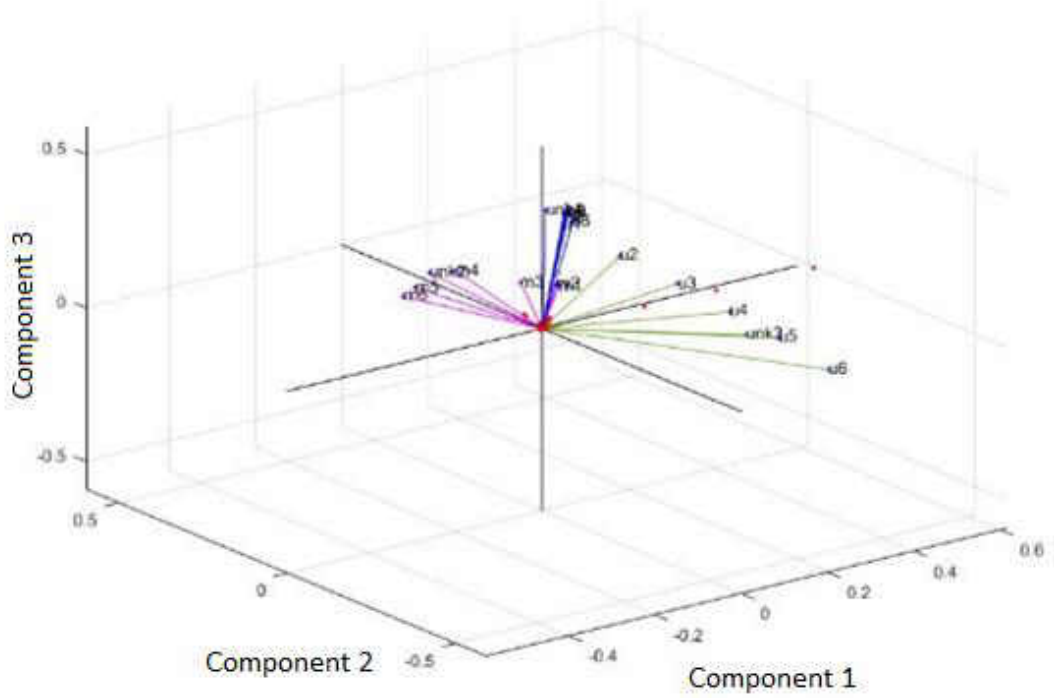

Figure 5.10: Accelerometer 4, 3 dimensional PCA.

Based on the data presented in figures 5.7 through 5.10, it can be concluded that PCA is capable of detecting mechanical faults based on the processed vibration data. Within the loadings plot of each graph, each of the fault conditions can be seen grouped together with other points of the same fault type. It is clear from these figures that with the third principal component added into consideration the data patterns are distinguished more precisely.

As for the score data, there is less transparency about the information shown compared to the loading plot. This is because each point represents a single amplitude value with respect to each data set. Within figures 5.7-5.10, the addition of a third PC dimension shows a distinct improvement in the grouping of each fault condition. Compared to the previous graphs involving only two PC dimensions, the misaligned and

healthy groups in figures 5.7-5.10 do not lie within the same region. Instead, each fault group becomes more distinct with the addition of a third PC dimension and would be easier to recognize computationally. This concept is explained further by the incorporation of unknown data sets in each fault grouping.

Considering figures 5.7-5.10, the unknown data sets, represented by unk1-unk3, can be seen near or within each fault group. This proves that the unknown situations can be precisely identified using principal components analysis.

In summary, PCA can be used to distinguish between motor faults of varying types. This, of course, is done in conjunction with several accelerometers as the use of supplementary data can provide a more in-depth look at the data. By comparing data from multiple accelerometers, steps can be taken towards automating the fault identification process. This is further supported by the similarities between the unknown data set and the other fault tests. Additionally, when dealing with a system running at a constant speed, the data has shown a correlation between the faulty data set's severity and its respective position in the PCA graph. Meaning that the fault severity of an unknown data set could be potentially estimated. With that said, PCA provides a simple and inexpensive alternative to current maintenance techniques. Not only can industries become more efficient by reducing production costs, but they may also see an increase in productivity by avoiding unplanned plant shutdowns thus improving the industry as a whole.

5.3 Singular Value Decomposition

Another method investigated for fault classification, is singular value decomposition. This approach follows similar path as principal components analysis. This method is commonly used in signal processing and statistics. Basically, SVD is a more general model of PCA. In order to get the PCA plots, the mean value of the vibration amplitudes is calculated and then subtracted from the amplitudes. The resulting value is then divided buy the standard deviation of the original vibration data. In many applications the features ought to be detected have positive values, whether it's the intensity of a pixel or the maximum vibration's amplitude. Typically, the remarkable features that can be used in the classification scheme, have higher magnitudes. In PCA, when the mean is subtracted, the uninteresting insignificant amplitudes get a negative value, in some cases, possibly with high magnitudes. In other words, the unimportant features are now identified as the key features used for classification. This is the most significant difference between PCA and SVD. However, in this study the mean value is very close to zero and does not slightly affect the vibration data. Therefore, in this case, SVD achieves same results as the PCA.

5.4 K-Nearest Neighbor

In this section a fault detection and classification technique for the faulty conditions of misaligned shaft and unbalanced rotor is presented. This method is based on vibration analysis and K-Nearest Neighbor (KNN) classifiers. In KNN method used, the output is a class membership belonging to one of the health conditions of the machine. An unknown

dataset will be classified based on a majority vote of its neighbors. KNN method is considered as the simplest of all machine learning algorithms.

In this method the Euclidean distance is calculated for to define the category in which the unknown condition falls in. This method can also be used for severity estimations. However, it relies heavily on the training dataset and therefore it is recommended to have a very large training data set to avoid the errors raised from noisy measurements.

The training dataset for KNN is generated through controlled predetermined amount of unbalanced load and misalignment at different levels, as well as ideal situation. The key features are selected based on the characteristic frequencies derived from spectrum analysis. To improve classification accuracy, features selected from training dataset were weighted according to their influence levels on distinguishing fault types.

Considering there is an unknown vibration data shown in Table 5.1.

Table 5.1: An unknown vibration data

Feature 1	Feature 2	Feature 3	Feature 4	Feature 5	Feature 6	Situation
0.3401	0.0035	0.0022	0.0034	0.002	0.0014	Unknown

Table 5.2 displays the vibration amplitudes of the training data sets used in principal components analysis. It is demonstrated how an unknown data set is categorized based on the trained data.

Table 5.2: Vibration dataset for KNN analysis

Feature1	Feature2	Feature3	Feature4	Feature5	Feature6	Rank	Euclidean Distance	Category
0.0463	0.0041	0.0048	0.0028	0.0013	0.0022	11	0.197087	Health
0.0461	0.0041	0.0045	0.0025	0.0009	0.0022	12	0.197221	Health
0.0465	0.0041	0.0049	0.0021	0.0012	0.0021	9	0.196953	Health
0.0465	0.0041	0.0051	0.0032	0.0015	0.0021	10	0.196953	Health
0.0474	0.0042	0.0049	0.0023	0.001	0.0021	8	0.196349	Health
0.0507	0.0041	0.0052	0.0025	0.0011	0.0022	7	0.194136	Health
0.1517	0.0025	0.0047	0.0024	0.0015	0.0024	4	0.126383	Unbalance
0.0724	0.0034	0.0048	0.0022	0.0014	0.002	6	0.179579	Unbalance
0.2734	0.0047	0.0066	0.0035	0.0018	0.0026	1	0.04475	Unbalance
0.2048	0.001	0.0046	0.0023	0.0017	0.0022	3	0.090762	Unbalance
0.1129	0.0028	0.0039	0.0027	0.0013	0.0024	5	0.152411	Unbalance
0.2423	0.0028	0.0056	0.0022	0.0021	0.0024	2	0.065608	Unbalance
0.0419	0.0065	0.0037	0.005	0.002	0.0067	17	0.200064	Misalignment
0.0432	0.0065	0.0035	0.0052	0.0012	0.0034	15	0.199169	Misalignment
0.0429	0.0061	0.0048	0.0053	0.0017	0.0045	16	0.199375	Misalignment
0.0411	0.0067	0.0037	0.0037	0.0029	0.0063	18	0.200596	Misalignment
0.0453	0.0033	0.0024	0.0041	0.0012	0.0033	13	0.197761	Misalignment
0.044	0.0052	0.0022	0.0034	0.002	0.0014	14	0.198632	Misalignment

Table 5.2 demonstrates how an unknown health condition can be determined based on KNN analysis. The Euclidean distances are calculated for the unknown vibration data and the trained dataset, and then the distances were ranked to find the closest distance to the unknown situation. The highlighted vibration data has the lowest distance. Therefore, the unknown situation is classified as unbalanced.

5.5 Chapter Summary

In this chapter, the statistical methods used in machine learning algorithms are implemented to classify the failure type automatically. For this purpose, principal components analysis, singular value decomposition, and K-nearest neighbor approach were investigated. The results verified that these simple models have provided an inexpensive and cohesive method for failure detection and categorization.

For rotating machines fault classification based on vibration data, PCA has provided the most valuable information. KNN relies heavily on the trained data and cannot be used to estimate the faults severity. Moreover, there is no need for feature extraction in PCA which enables this method to become more general in identifying different faulty situations even if the faulty condition does not lie within the trained dataset.

CHAPTER 6

CONCLUSIONS AND FUTURE WORK

6.1 Conclusions and Discussions

Vibration analysis is a multipart discipline that helps increase quality, reliability and cost efficiency in so many different industries, including but not limited to electric machines manufacturing, automobile industries, aerospace, transportation, medical and etc. Analyzing and addressing typical vibration problems requires a basic knowledge of theoretical models, time and frequency domain analysis, measurement techniques and equipment, vibration suppression techniques, and modal analysis. Although the theory of frequency response analysis on the data acquired by accelerometer sensors and vibration measurement apparatus has been studied since the advent of accelerometer sensors. However, these methodologies have yet to gather into a single tool in the hands of an electro-mechanical technician in industry to perform complex diagnostic analysis. Therefore, the efforts of this project were focused on performance analysis of a rotating machine using its vibration profile.

In this thesis, vibration responses of different faulty conditions were investigated. The faults studied include: Unbalanced rotor condition, shaft misalignment, damaged stator's wirings, damaged bearings, and mechanical looseness. An induction motor's

vibrations were measured and analyzed using fast Fourier transform signal processing method. The characteristic frequencies which are considered as the signature response of the faulty conditions were revealed. Next, the correction methods for the faulty conditions were discussed. An automatic balancing method based on computer vision applications was developed. Finally, using statistical approaches from machine learning algorithms the faults were classified based on their signature responses and their severities.

In this project, the validity of the results obtained through vibration measurement have been proven and verified as an effective diagnostic and prognostic tool for failure modes of any critical parts in a system (in this study it was specifically applied on electrical rotating machines).

6.2 Future Work

As a continuation of this research, the possibility of application of Artificial Intelligence (AI) and machine learning on evaluation of big data captured by the sensors or the sensory network on the rotating devices could facilitate the failure mode analysis and predictions on moving mechanical systems and parts. Moreover, the findings assorted in this project along with the data analysis tool can come together to form a handheld prototype that can be used in industry for health monitoring of any equipment and instrumentation of this type.

The data obtained from this methodology can be expanded to lifetime estimation (End of life prediction), failure modes and effects analysis (FMEA), reliability tests, standard compliance test (ISO 1940/ANSI S2-19), and etc.

New monitoring methods are being developed based on the advancements is machine vision technologies. The methods can be used to correct other faults such as misalignment. It is estimated that with developments in cameras, and image processing methods, the monitoring techniques will move toward failure analysis based on the captured videos of the rotating machines.

References

[1] Plante, T., Nejadpak, A., & Yang, C. X. (2015, November). Faults detection and failures prediction using vibration analysis. In *IEEE AUTOTESTCON, 2015* (pp. 227-231). IEEE.

[2] Schoukens, J., Pintelon, R., & Van Hamme, H. (1992). The interpolated fast Fourier transform: A comparative study. *IEEE Transactions on Instrumentation and Measurement*, *41*(2), 226-232.

[3] Cohen, L. (1995). *Time-frequency analysis* (Vol. 778). Englewood Cliffs, NJ:: Prentice Hall PTR.

[4] Nejadpak, A., & Yang, C. X. (2016, May). A vibration-based diagnostic tool for analysis of superimposed failures in electric machines. In *Electro Information Technology (EIT), 2016 IEEE International Conference on* (pp. 0324-0329). IEEE.

[5] http://www.ni.com/white-paper/3807/en/

[6] Nandi, S., Toliyat, H. A., & Li, X. (2005). Condition monitoring and fault diagnosis of electrical motors—A review. *IEEE transactions on energy conversion*, *20*(4), 719-729.

[7] Rao, B. K. N. (1996). *Handbook of condition monitoring*. Elsevier.

[8] Randall, R. B. (2011). *Vibration-based condition monitoring: industrial, aerospace and automotive applications*. John Wiley & Sons.

[9] Scheffer, C., & Girdhar, P. (2004). *Practical machinery vibration analysis and predictive maintenance*. Elsevier.

[10] Randall, R. B. (2004). State of the art in monitoring rotating machinery-part 1. *Sound and vibration*, *38*(3), 14-21.

[11] Patel, T. H., & Darpe, A. K. (2009). Experimental investigations on vibration response of misaligned rotors. *Mechanical Systems and Signal Processing*, *23*(7), 2236-2252.

[12] Hariharan, V., & Srinivasan, P. S. S. (2011). Vibration analysis of parallel misaligned shaft with ball bearing system. *Sonklanakarin Journal of Science and Technology*, *33*(1), 61.

[13] Lim, G. M., Bae, D. M., & Kim, J. H. (2014). Fault diagnosis of rotating machine by thermography method on support vector machine. *Journal of Mechanical Science and Technology*, *28*(8), 2947-2952.

[14] Tandon, N., & Choudhury, A. (1999). A review of vibration and acoustic measurement methods for the detection of defects in rolling element bearings. *Tribology international*, *32*(8), 469-480.

[15] Baydar, N., & Ball, A. (2003). Detection of gear failures via vibration and acoustic signals using wavelet transform. *Mechanical Systems and Signal Processing*, *17*(4), 787-804.

[16] Loutas, T. H., Roulias, D., Pauly, E., & Kostopoulos, V. (2011). The combined use of vibration, acoustic emission and oil debris on-line monitoring towards a more effective condition monitoring of rotating machinery. *Mechanical systems and signal processing*, *25*(4), 1339-1352.

[17] Mehala, N. (2010). Condition monitoring and fault diagnosis of induction motor using motor current signature analysis. *A Ph. D Thesis submitted to the Electrical Engineering Department, National Institute of Technology, Kurushetra, India*.

[18] Plante, T., Stanley, L., Nejadpak, A., & Yang, C. X. (2016, September). Rotating machine fault detection using principal component analysis of vibration signal. In *IEEE AUTOTESTCON, 2016* (pp. 1-7). IEEE.

[19] Lachouri, A., Baiche, K., Djeghader, R., Doghmane, N., & Ouhtati, S. (2008, April). Analyze and fault diagnosis by multi-scale PCA. In *Information and communication technologies: From theory to applications, 2008. ICTTA 2008. 3rd International Conference on* (pp. 1-6). IEEE.

[20] Glowacz, A. (2014). Diagnostics of synchronous motor based on analysis of acoustic signals with the use of line spectral frequencies and K-nearest neighbor classifier. *Archives of Acoustics*, *39*(2), 189-194.

[21] Lei, Y., & Zuo, M. J. (2009). Gear crack level identification based on weighted K nearest neighbor classification algorithm. *Mechanical Systems and Signal Processing*, *23*(5), 1535-1547.

[22] Safizadeh, M. S., & Latifi, S. K. (2014). Using multi-sensor data fusion for vibration fault diagnosis of rolling element bearings by accelerometer and load cell. *Information Fusion*, *18*, 1-8.

[23] Yang, D. M., Stronach, A. F., & MacConnell, P. (2003). The application of advanced signal processing techniques to induction motor bearing condition diagnosis. *Meccanica*, *38*(2), 297-308.

[24] Ruotolo, R., & Surace, C. (1999). Using SVD to detect damage in structures with different operational conditions. *Journal of Sound and Vibration*, *226*(3), 425-439.

[25] Saxena, A., & Saad, A. (2007). Evolving an artificial neural network classifier for condition monitoring of rotating mechanical systems. *Applied Soft Computing*, *7*(1), 441-454.

[26] Rafiee, J., Arvani, F., Harifi, A., & Sadeghi, M. H. (2007). Intelligent condition monitoring of a gearbox using artificial neural network. *Mechanical systems and signal processing*, *21*(4), 1746-1754.

[27] Samanta, B., & Al-Balushi, K. R. (2003). Artificial neural network based fault diagnostics of rolling element bearings using time-domain features. *Mechanical systems and signal processing*, *17*(2), 317-328.

[28] Zhang, L., Xu, J., Yang, J., Yang, D., & Wang, D. (2008). Multiscale morphology analysis and its application to fault diagnosis. *Mechanical Systems and Signal Processing*, *22*(3), 597-610.

[29] Elgharib, M., Hefeeda, M., Durand, F., & Freeman, W. T. (2015). Video magnification in presence of large motions. In *Proceedings of the IEEE Conference on Computer Vision and Pattern Recognition* (pp. 4119-4127).

[30] Wadhwa, N., Rubinstein, M., Durand, F., & Freeman, W. T. (2013). Phase-based video motion processing. *ACM Transactions on Graphics (TOG)*, *32*(4), 80.

[31] Wu, H. Y., Rubinstein, M., Shih, E., Guttag, J., Durand, F., & Freeman, W. (2012). Eulerian video magnification for revealing subtle changes in the world.

[32] Davis, A., Bouman, K. L., Chen, J. G., Rubinstein, M., Durand, F., & Freeman, W. T. (2015). Visual vibrometry: Estimating material properties from small motion in video. In *Proceedings of the IEEE Conference on Computer Vision and Pattern Recognition* (pp. 5335-5343).

[33] Pickens, S. (2007). Vibration Trouble-shooting Field Guide. *PDM Engineering*.

[34] Graney, B. P., & Starry, K. (2012). Rolling element bearing analysis. *Materials Evaluation*, *70*(1), 78.

[35] Copping, M., "Vibration analysis reporting–bearing failure stages and responses", *Reliabilityweb.com*. 2015.

[36] Southwick, D. (1993). Using full spectrum plots. *Orbit*, *14*(4), 12-16.

[37] Southwick, D. (1994). Using full spectrum plots part 2. *Orbit,* Vol. 15, No.2, 1994. Bently Nevada Corporation

[38] Cruz, S. M., & Cardoso, A. M. (2001). Stator winding fault diagnosis in three-phase synchronous and asynchronous motors, by the extended Park's vector approach. *IEEE Transactions on industry applications*, *37*(5), 1227-1233.

[39] An engineers guide to shaft alignment, vibration analysis, dynamic balancing & wear debris analysis, handbook, PRUFTECHNIK LTD, 2002

[40] Dynamic balancing of Rotating Machinery Experiment. Technical Advisor: Dr. K. Nisbett. January 1996.

[41] Canny, J. (1986). A computational approach to edge detection. *IEEE Transactions on pattern analysis and machine intelligence*, (6), 679-698.

[42] Gao, W., Zhang, X., Yang, L., & Liu, H. (2010, July). An improved Sobel edge detection. In *Computer Science and Information Technology (ICCSIT), 2010 3rd IEEE International Conference on* (Vol. 5, pp. 67-71). IEEE.

[43] Shrivakshan, G. T., & Chandrasekar, C. (2012). A comparison of various edge detection techniques used in image processing. *IJCSI International Journal of Computer Science Issues*, *9*(5), 272-276.

[44] Duda, R. O., & Hart, P. E. (1972). Use of the Hough transformation to detect lines and curves in pictures. *Communications of the ACM*, *15*(1), 11-15.

[45] Willson, R. G. (1994, October). Modeling and calibration of automated zoom lenses. In *Photonics for Industrial Applications* (pp. 170-186). International Society for Optics and Photonics.

[46] Xia, Z., Xia, S., Wan, L., & Cai, S. (2012). Spectral regression based fault feature extraction for bearing accelerometer sensor signals. *Sensors*, *12*(10), 13694-13719.

[47] Powell, V., & Lehe, L. (2015). Principal component analysis explained visually. *DISQUS, Available: http://setosa. io/ev/principal-component-analysis/.[Accessed 11 July 2016]*.

[48] J. Starmer, StatQuest: Principle Component Analysis (PCA) clearly explained, 2015.

[49] Smith, L. I. (2002). A tutorial on principal components analysis. *Cornell University, USA*, *51*(52), 65.